

Single Layer Single Gradient Unlearning

Zikai Cai Yaoteng Tan M. Salman Asif
University of California Riverside
zcaio32@ucr.edu ytan073@ucr.edu sasif@ucr.edu

Abstract

Machine unlearning methods seek to revise pretrained models such that effects of certain training samples can be removed. In addition to effective erasure, low computational cost and general utility retention are also highly desirable. Existing unlearning methods usually involve iterative updates over the model parameters, which incurs a high computational cost. In this work, we propose an efficient method that only requires a one-time gradient computation, with which we modify only a single layer of model parameters. Specifically, we first identify a small number of model layers that lie on the Pareto front of high forget importance and low retain influence as critical layers. Then we search for a suitable step size and take a step along the gradient direction of a single critical layer while keeping other layers frozen. This method is highly modular and can be used to unlearn multiple concepts simultaneously in a controllable manner. We demonstrate the effectiveness and efficiency of this method on various models including CLIP, stable diffusion, and VLMs, surpassing other state-of-the-art methods.

1 Introduction

Modern machine learning models, including large language models (LLMs) [37, 38, 4, 3, 24], Stable Diffusion (SD) [39, 40, 35, 47], and vision language models (VLMs) [50, 28, 27, 26] leverage vast amounts of data for training. Large-scale web scrapers, such as [Common Crawl](#), archive billions of webpages monthly, providing massive data sources to train such revolutionary AI models. While these large unsupervised datasets significantly enhance performance under scaling law [20], they also raise serious data privacy and legal compliance [1] concerns. For instance, researchers [44] discovered hundreds of URLs linked to child sexual abuse material in LAION-5B [41], a popular dataset used to train stable diffusion. Consequently, the dataset was taken offline, and associated models are now subject to safety investigations. Completely abandoning previously trained model weights and retraining large models from scratch using scrutinized dataset is prohibitively expensive, highlighting the need for efficient data removal methods.

Machine unlearning [5, 32, 2, 17, 14, 7, 16, 15, 9, 23, 19, 43, 10, 11, 48, 29, 25], a technique designed to reverse the learning process, aims to efficiently remove specific data points from a trained model without the need of retraining from scratch, has been gaining increasing attention as a solution to the challenges posed by data privacy and legal compliance issues in modern AI training processes. Its objective is threefold. First, low computational cost, as the naïve approach of training from scratch achieves the best result (exact unlearning), but is expensive. Second, effective unlearning, ensuring that the model forgets the intended data completely. Third, utility retention, maintaining its performance on tasks unrelated to the forgotten data. However, current unlearning methods

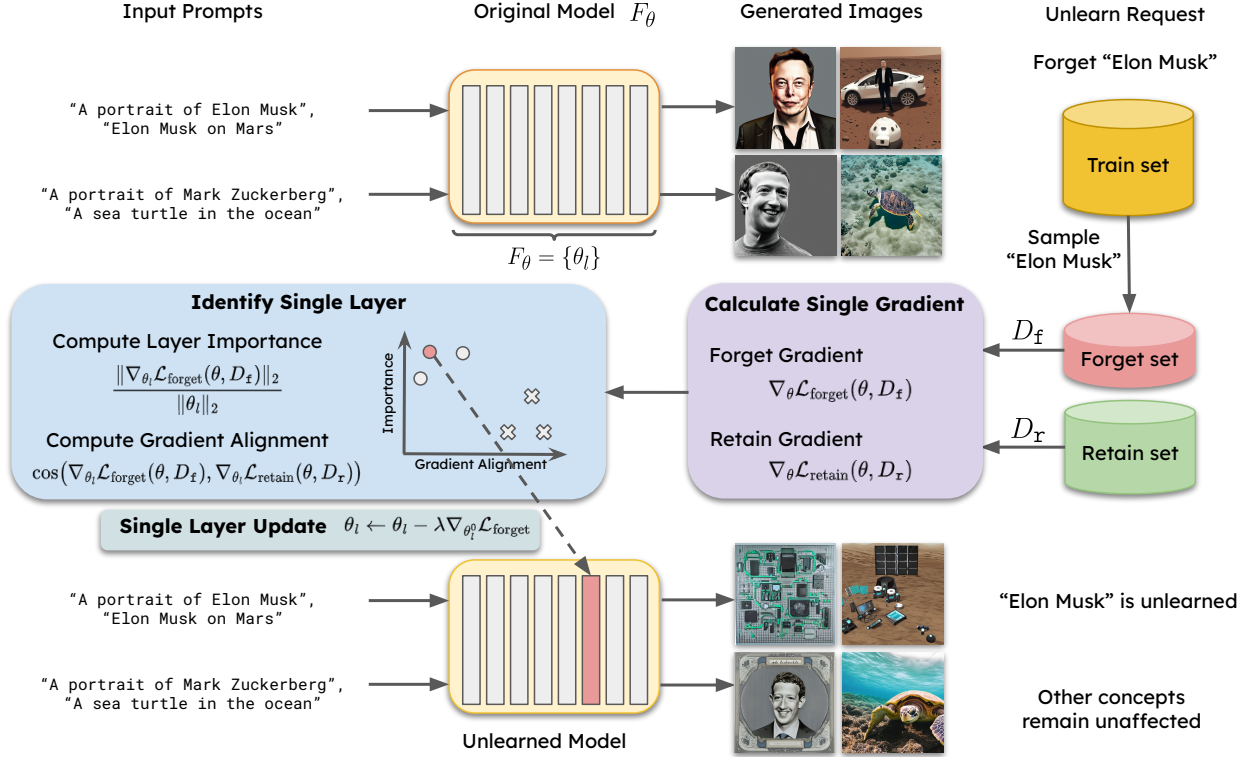


Figure 1: Overview of our framework. Given an unlearning query, such as removing an identity like Elon Musk, we first curate or generate a forget set containing relevant data and a retain set with data points we want to preserve. Using these datasets, we calculate and store the model gradients. Based on these gradients, we identify the important layers to update for unlearning. We then take a step along the forget gradients of a single layer and evaluate the model’s unlearning performance. To determine a suitable step size λ , we employ a binary search. After unlearning, the specified concepts are effectively erased while retaining the model’s overall utility.

often fall short. They usually involve iterative updates over the model parameters, resulting in high computational costs. Additionally, achieving a balance between effective unlearning and utility retention remains a challenge.

In this paper, we push the boundaries of efficiency with an algorithm that requires only a single gradient calculation and updates a single layer to achieve effective unlearning without affecting the model’s general utility. We first calculate gradients of forget and retain losses with respect to model weights using a designated or curated forget and retain set. Based on these gradients, we propose two metrics, namely layer importance and gradient alignment, to select the appropriate layers for unlearning. To determine a suitable step size for weight updates, our method employs an efficient binary search along the direction of forget gradients. We demonstrate that our method outperforms state-of-the-art methods in unlearning tasks involving CLIP models, stable diffusion and VLMs, across various tasks and architectures. In addition to its efficiency and effectiveness, our methods offers higher modularity and better interpretability. Specifically, we can calculate the gradients of different unlearning tasks independently and unlearn them simultaneously. By assigning different layers for different unlearning tasks, we avoid interference. Our layer selection approach provides

insights into the features learned by different layers and their functionalities, offering generalized guidance for new tasks and model architectures without additional computation.

2 Background

In this section, we present background knowledge on machine unlearning and vision-language alignment using CLIP, which is the primary focus of this paper.

2.1 Machine unlearning preliminaries

One of the core objectives of machine unlearning is to remove the influence of a specific subset of training data D , on a pre-trained model, represented as $F_\theta(D)$ with model parameters represented as θ . Let us assume $D_f \subset D$ denotes the subset selected for unlearning (forgetting). The primary challenge is to ensure that the unlearning process is computationally efficient, significantly reducing the time and resources compared to retraining the model from scratch with the remaining dataset $D_r = D \setminus D_f$. The ideal unlearning algorithm, which we refer to as U , should yield an unlearned model $U(F_\theta(D), D, D_f)$ with model parameters θ_f that is functionally indistinguishable from a model retrained exclusively on the retain set $F_{\theta_f}(D_r)$. The main objective is captured in Eqn. 1, where N denotes the number of elements in the dataset D , α is the balancing factor, (x, y) is an element from the dataset, and ℓ is the loss function, usually the training loss.

$$\min_{\theta} \underbrace{\frac{1}{N_r} \sum_{(x_r, y_r) \in D_r} \ell(F_\theta(x_r), y_r)}_{\mathcal{L}_{\text{retain}}} - \underbrace{\frac{\alpha}{N_f} \sum_{(x_f, y_f) \in D_f} \ell(F_\theta(x_f), y_f)}_{\mathcal{L}_{\text{forget}}} \quad (1)$$

Naïve gradient ascent (GA) solely on the forget set (minimizing the second term in Eqn. 1) is effective at increasing forget loss but is prone to over-unlearning, which can significantly reduce test accuracy if iterations exceed an appropriate limit. Fine tuning (FT), which only uses the retain set (minimizing the first term in Eqn. 1), is ineffective at forgetting. However it can be combined with GA in a two-stage training paradigm [10] to mitigate over-unlearning. We refer to this two-stage framework, involving GA and FT, as GAFT (Eqn. 1).

Recent works[10, 11] have focused on identifying salient parameters via gradient calculation to stabilize unlearning by updating only these parameters while keeping the rest of the model intact. Specifically, SalUn [10] uses hard thresholds on the gradient of forgetting loss with respect to model weights, updating only those weights with gradient magnitudes higher than a certain threshold (e.g., the median gradient magnitude across the model). SSD[11] proposes dampening model weights that are disproportionately important to the forget and retain sets, scaling down the values of such weights. While these methods achieve localized editing and improve overall unlearning performance, the significant weights are spread throughout the model, which does not offer understanding about the structure of the model. They also require careful hyperparameter tuning, including learning rate, the number of iterations, and hyperparameters for selecting suitable masks for saliency approaches. All these limitations motivate us to develop a method that is hyperparameter-free and easily interpretable.

2.2 Vision language alignment

Existing methods in machine unlearning often suffer from high computational costs and limited scalability, primarily focusing on small-scale image classification models [19, 11]. In contrast, our method demonstrates superior scalability and versatility, making it applicable to large multi-modal foundation models such as CLIP[36], stable diffusion [39], and visual language models (VLMs) [28]. CLIP models, in particular, play a central role in driving the development of various multi-modal models by aligning visual and textual representations through a contrastive loss function [8].

$$\ell = \frac{1}{2N} \sum_{i=1}^N (\ell_{i2t}(i) + \ell_{t2i}(i)), \quad (2)$$

$$\ell_{i2t}(i) = -\log \frac{\exp(\cos(\mathbf{v}_i, \mathbf{t}_i)/\tau)}{\sum_{j=1}^N \exp(\cos(\mathbf{v}_i, \mathbf{t}_j)/\tau)}, \quad \ell_{t2i}(i) = -\log \frac{\exp(\cos(\mathbf{t}_i, \mathbf{v}_i)/\tau)}{\sum_{j=1}^N \exp(\cos(\mathbf{t}_i, \mathbf{v}_j)/\tau)}. \quad (3)$$

Here \mathbf{v}_i is the normalized embedding of image x_i through the vision model f_v and \mathbf{t}_i is the normalized embedding of text y_i through the text model f_t . The temperature τ controls the sharpness of the probability distribution after softmax. Cosine similarity between \mathbf{v}_i and \mathbf{t}_j is defined as $\cos(\mathbf{v}_i, \mathbf{t}_j) = \mathbf{v}_i \cdot \mathbf{t}_j$.

By minimizing the contrastive loss in Eqn. 2, the model learns to align vision and language information of the same pair in the embedding space. In unlearning, we break such alignments.

3 Unlearning via weight arithmetic

Our approach improves the state-of-the-art along three axes: (1) low computational cost (achieved through a single gradient calculation followed by weight arithmetic), (2) effective unlearning (by identifying layers with high importance to the forget set), and (3) high retention of general utility (via pinpointing layers with low gradient alignment to the retain set). The framework is illustrated in Figure 1.

3.1 Loss functions for gradient calculation

It is important to select appropriate loss functions to perform unlearning. For image classification models, cross-entropy loss can be directly used as both retain loss and forget loss. However, the scenario is different for contrastive learning. For the retain set, we can still use the original contrastive loss as in Eqn. 2.

$$\mathcal{L}_{\text{retain}} = \frac{1}{2N} \sum_{i=1}^N (\ell_{i2t}(i) + \ell_{t2i}(i)), \quad (4)$$

However, for the forget set, we employ the cosine embedding loss (Eqn. 5) instead since it directly pushes the embeddings of positive pairs away while not tampering with the embeddings of negative pairs.

$$\mathcal{L}_{\text{forget}}(\mathbf{v}_i, \mathbf{t}_j) = 1 - \cos(\mathbf{v}_i, \mathbf{t}_j) \quad (5)$$

Using the original contrastive loss as forget loss will result in ineffective unlearning.

3.2 Layer identification

In this work, we are inspired by the distinct feature representations learned by different layers within deep networks [49, 34, 13]. For example, early layers in vision models generally extract basic features such as edges and textures, while later layers discern more specific details. To target unlearning effectively, we aim to modify only those layers that hold information directly relevant to the unlearning objectives, rather than those that process abstract features which could be learned independently of the examples to be forgotten. Our primary goal is to pinpoint the layers most critical to the specific unlearning task, ensuring that adjustments lead to desired outcomes without needless alterations to unrelated functionalities. Moreover, maintaining the overall utility of the model is paramount; hence, we endeavor to perform unlearning within the “nullspace” of the retain set. This strategy involves identifying layers that have minimal impact on the performance of retained data while effectively facilitating the unlearning of selected features. This method not only enhances the precision of the unlearning process but also provides greater interpretability and a clearer insight into how unlearning and data retention are managed within the network.

Similar to [11], we leverage Fisher information matrix [21, 18, 22] to measure the effect of each parameter on the objective. Calculating the exact Fisher information matrix requires obtaining the second-order derivative of the model output with respect to its parameters, which is computationally prohibitive. To make the computation more tractable, we use the diagonal approximation:

$$\mathcal{I}_D(\theta) = -\mathbb{E} \left[\frac{\partial^2}{\partial \theta^2} \log L(\theta; D) \right] = \mathbb{E} \left[\left(\frac{\partial}{\partial \theta} \log L(\theta; D) \right) \left(\frac{\partial}{\partial \theta} \log L(\theta; D) \right)^T \right]. \quad (6)$$

The diagonal elements of the Fisher Information Matrix quantify the sensitivity of the log-likelihood function to changes in individual parameters. To extend this to layers, we aggregate these sensitivities at the layer level. For a layer l , the importance of the layer is measured by aggregating the ratio of the ℓ_2 norm of the forget loss gradients to the ℓ_2 norm of the parameters within the layer as

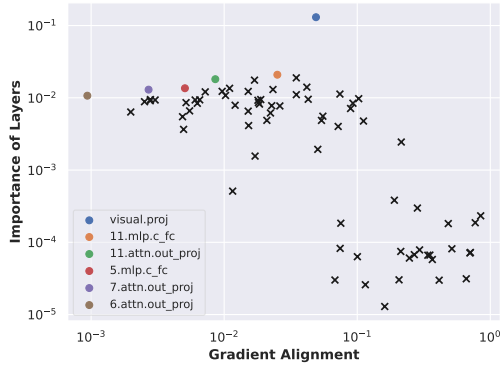
$$\text{Importance of layer } l: \quad \text{Importance}(l) = \frac{\sqrt{\mathcal{I}_{D_f}(\theta_l)}}{\|\theta_l\|_2} = \frac{\|\nabla_{\theta_l} \mathcal{L}_{\text{forget}}(\theta, D_f)\|_2}{\|\theta_l\|_2}. \quad (7)$$

Using the importance criteria alone is not sufficient, as it only indicates which layer can influence the forget set. For layer selection, we prefer layers for which the forget gradients are orthogonal to the retain gradients by computing

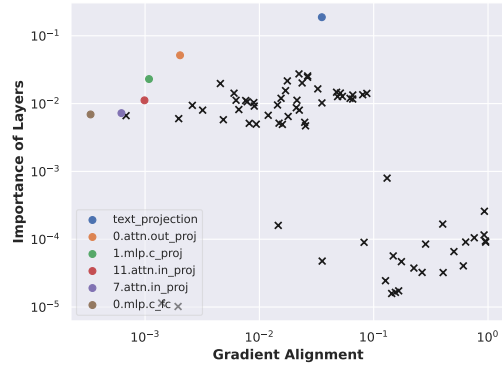
$$\text{Gradient alignment:} \quad \text{Alignment}(l) = \cos(\nabla_{\theta_l} \mathcal{L}_{\text{forget}}(\theta, D_f), \nabla_{\theta_l} \mathcal{L}_{\text{retain}}(\theta, D_r)). \quad (8)$$

This ensures that updates for unlearning the forget set do not adversely affect the retain set.

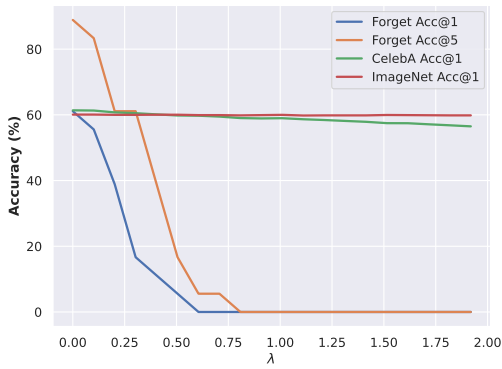
To identify important layers, we use the ratio of the ℓ_2 norm of the forget loss gradients to the ℓ_2 norm of the layer parameters as the importance measure, and ensure orthogonality of the forget gradients to the retain gradients to maintain performance on the retain set. To balance these objectives, we utilize the concept of Pareto optimal set [31], which represents a set of optimal solutions with a trade-off in two objectives. In our context, the two objectives are maximizing the importance measure and ensuring the orthogonality condition. We present an experimental result in Figure 2 to illustrate the Pareto front for unlearning a person identify from CLIP ViT-B-32. The layers on the top left are the ones that unlearn the forget set without affecting the retain set.



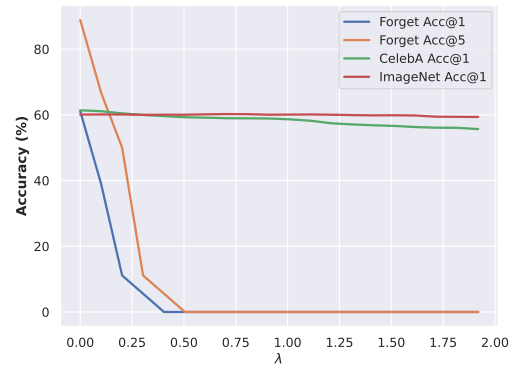
(a) Layers of vision model



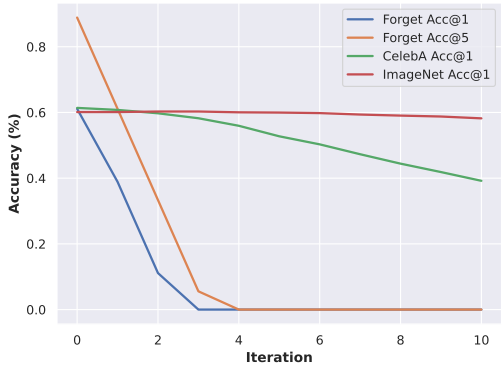
(b) Layers of language model



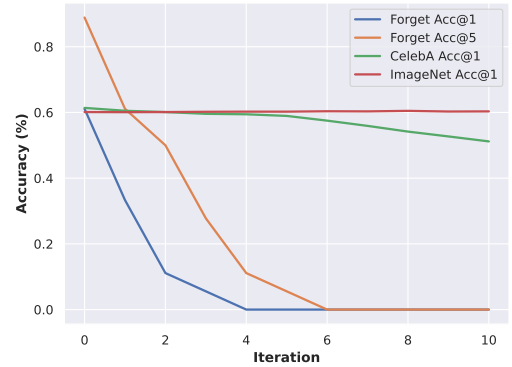
(c) Unlearn single vision layer



(d) Unlearn single language layer



(e) GA on whole model



(f) GAFT on whole model

Figure 2: The first row shows scatter plots of layers within (a) vision and (b) language models from CLIP ViT-B-32 trained on Laion-400M dataset. Layers on Pareto front for unlearning an identity (e.g. Elon Musk) are marked as dots in different colors, while less significant layers are marked as crosses in black. The second row demonstrates the unlearning performance when moving along the direction of forget gradient (with step size λ) on a single (c) vision layer `11.attn.out_proj` and (d) language layer `0.attn.out_proj`. Our method precisely identifies a small number of significant layers within the entire model and efficiently unlearns without significantly compromising utility. Additional examples of different identities, models, and layers are provided in Figures 9, 13, and 14 respectively. The third row shows the performance of (e) GA and (f) GAFT on the whole model, illustrating that iterative gradient calculations are not superior to a single gradient step.

3.3 Linearizing unlearning trajectory

Existing approaches for unlearning calculate gradients at each iteration for updating the model parameters, which adds to computational complexity. In this work, we observe that calculating gradients repeatedly is unnecessary. Instead, we only perform one gradient calculation for the initialized model and update the parameters, θ_l for any layer l , in a weight arithmetic manner. That is, update the weights along a fixed gradient direction at every iteration as

$$\theta_l \leftarrow \theta_l - \lambda \nabla_{\theta_l} \mathcal{L}_{\text{forget}}, \quad (9)$$

where $\nabla_{\theta_l} \mathcal{L}_{\text{forget}}$ represents the gradient computed at the first iteration. This can be regraded as linearizing the unlearning trajectory. Combined with our previous discussion on important layer identification, this method is sufficient in unlearning while retaining general performance. For selecting the step size, we perform a binary search along the linearized trajectory, and stop whenever appropriate as suggested by the evaluation metric.

3.4 Generalization to stable diffusion and VLMs

By harnessing the capability of effective unlearning in CLIP models, we can extend this technique to edit larger and more powerful models that rely on CLIP, including image generation models such as stable diffusion [39, 40]) and VLMs like LLaVA [28, 27]).

Unlearn stable diffusion. Diffusion models are popularized by their strong ability to generate high quality images based on text descriptions [33, 39]. The text prompt is first embedded into a high-dimensional vector space using a pre-trained language model, for example the latest **Stable Diffusion v2** model uses CLIP ViT-H/14 text encoder. Then the text conditioning is achieved through a cross-attention mechanism, where the text embedding guides each step of the denoising process. Starting from the initial noise \mathbf{x}_T , the iterative updates are performed as follows:

$$\mathbf{x}_{t-1} = \sqrt{\alpha_t} (\mathbf{x}_t - \gamma_t \nabla_{\mathbf{x}} \log p(\mathbf{x}_t | \mathbf{e})) + \sqrt{1 - \alpha_t} \mathbf{z}_t, \quad (10)$$

where \mathbf{x}_t is the noisy image at step t , \mathbf{z}_t is the noise added at step t , α_t is a time-dependent parameter controlling the noise balance, γ_t is the learning rate, $\mathbf{e} = f_t(\text{txt})$ is the text embedding, and $\nabla_{\mathbf{x}} \log p(\mathbf{x}_t | \mathbf{e})$ is the gradient of the log-probability of the noisy image given the text embedding, guiding the denoising process. We can keep the CLIP vision model frozen and only update the language model to achieve unlearning.

Unlearn VLMs. Vision-Language Models (VLMs) are at the forefront of AI research, enabling LLMs to process and understand multi-modal information. Recent work in LLaVA-1.5 [27] uses a pretrained CLIP visual encoder ViT-L/14-336px to extract the visual features $\mathbf{e} = f_v(\text{img})$. These visual features are then projected as a sequence of visual tokens into the word embedding space using an Multi-Layer Perceptron (MLP) denoted as \mathbf{W} . The visual tokens, $\mathbf{H}_v = \mathbf{W} \cdot \mathbf{e}$, are then concatenated with language tokens \mathbf{H}_q as input $\mathbf{H} = [\mathbf{H}_v; \mathbf{H}_q]$ to the language model to generate language response. The vision capability of VLMs hinges on the visual encoder. Therefore, by unlearning certain concepts from the CLIP vision model, we can influence the language model’s understanding and generation of responses.

4 Experiments

4.1 Experiment setup

Unlearning scenarios. Our experiments addressed two main types of unlearning scenarios for practical and generalizable impact: identity unlearning for privacy concerns and the unlearning of copyrighted content for compliance with legal standards. The focus was primarily on large scale multimodal models, including CLIP, stable diffusion, and VLMs.

Models and datasets. We employed various models in our experiments to demonstrate the broad applicability of our unlearning method. For CLIP models, we utilized architectures ranging from ViT-B-32 to EVA01-g-14, trained on LAION-400M dataset [42], and model weights sourced from the [OpenCLIP](#) repository [6]. For stable diffusion models, we opted for the latest version from [StabilityAI](#), which incorporates the CLIP-ViT-H-14 trained on the LAION-5B dataset. For VLMs, we tested the improved LLaVA-v1.5 model from [HuggingFace](#), which employs a CLIP ViT-L/14-336px model, trained by [OpenAI](#), as the visual extractor. To unlearn an identity, we curate the forget set by filtering the LAION-400M dataset to isolate image-text pairs specific to each identity. In our experiments, the number of filtered image-text pairs for each identity ranged from around 1k to 6k. For the retain set, we use a single shard of LAION-400M dataset, which typically consists of 10K images. However, due to expiring URL inks, we were only able to download approximately 7900 images from each shard. To assess the effectiveness of our unlearning method on various identities, we utilize the CelebA dataset [30], which features over 10K celebrities from diverse backgrounds. We sample 100 celebrities with high frequency in Laion-400M for evaluation. For evaluating the general utility of the models post-unlearning, we employ the ImageNet dataset.

Evaluation. We evaluate the unlearning performance using forget accuracy, i.e. zero-shot classification accuracy of unlearned contents. We follow the common zero-shot paradigm [36], where the prediction label of any given image is the text string whose text embedding is closest to the image embedding. For utility performance, we use zero-shot classification accuracy on ImageNet and CelebA dataset. Besides quantitative results, we also provide qualitative results of stable diffusion generated images before and after unlearning, question answering results of VLMs before and after unlearning.

Comparing methods. We compare with state-of-the-art methods along with classical methods. Specifically, we consider fine tuning (FT) [46], gradient ascent (GA) / negative gradient (NG) [45], saliency unlearning (SalUn) [10], selective synaptic dampening (SSD) [11] for CLIP zero-shot classification. For unlearning stable diffusion models, we compare with SalUn [10] and ESD [12].

4.2 Localizing layers and unlearning for CLIP

Our approach effectively pinpoints critical layers for updates, narrowing the search space from tens or hundreds of layers to just a few, as illustrated in Figures 2, 9 and 13. This strategy provides clear guidelines on which parts of the model to modify, revealing the distinct roles and mechanisms different layers serve in processing and integrating information within their respective architectures. We observe that, across different identities (see Figure 9) and architectures (see Figure 13), the final projection layers of both vision and language models are selected, due to their roles of transforming complex features extracted by the previous layers for making final predictions. We also observe that the late attention layers in vision models and early attention layers in language models. Vision transformers utilize attention mechanisms to focus on different parts of an image and aggregate

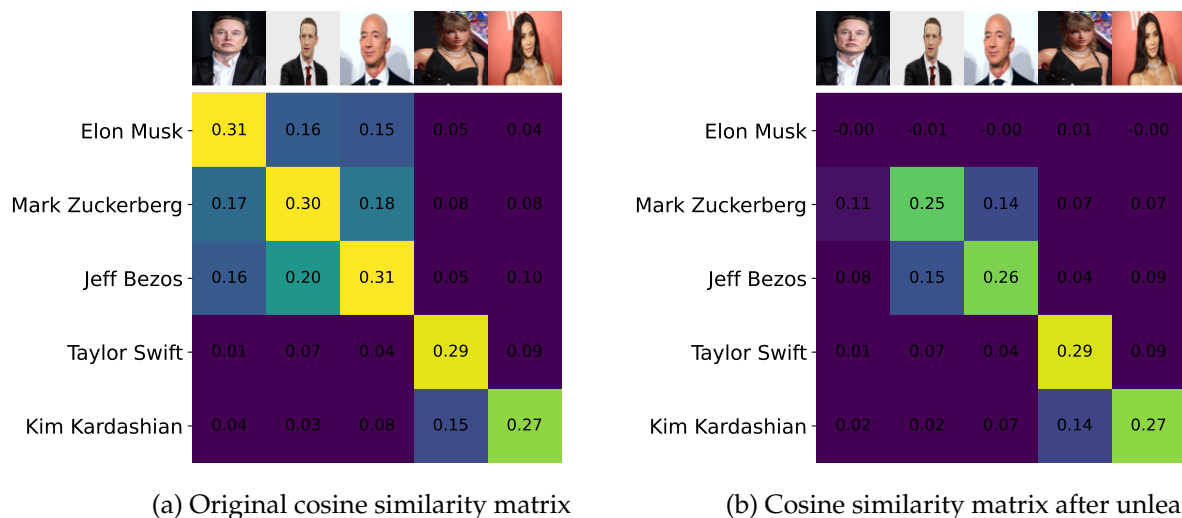


Figure 3: Cosine similarity matrix of image and text pairs before (a) and after (b) unlearning an identity - Elon Musk as an example. The original model can associate image and text of the same person with high cosine similarity. After unlearning, the image and text pair of Elon Musk are no longer matched, while other persons are only slightly affected. Here the 11th attention out projection layer of the vision model ViT-B-32 is unlearned.

contextual information from various spatial regions. The late attention layers in these models are closer to the output, thus more specialized in refining and utilizing contextually rich, high-level features. In contrast, language models often employ attention mechanisms right from the early layers to capture and process the sequential and contextual dependencies inherent in textual data. Early attention layers are crucial for establishing a foundational understanding of the language structure, including syntax and semantics. By focusing on early layers, modifications can influence the foundational processing of input text, effectively guiding the subsequent layers' interpretation and response to the content.

We demonstrate that modifying a single layer suffices to unlearn a concept while preserving the model's overall utility, as depicted in Figures 2, 3 and Table 1. It is noteworthy that the performance on unrelated tasks, like ImageNet for common object recognition, remains intact. However, for closely related tasks such as CelebA, which focuses on face recognition, there is a slight impact on performance. As shown in Table 1, our method outperforms other comparing methods on different metrics. In contrast, other methods require careful tuning of hyper-parameters, such as learning rate, to achieve a balance between unlearning effectiveness and utility preservation.

Table 1: Performance comparison of different unlearning methods on CLIP model. FA@1 and FA@5 represents the top-1 and top-5 forget accuracy (%), i.e. zero-shot classification accuracy of unlearned identity (average of 5 identities from Figure 3). TA_IN@1 and TA_CA@1 stands for the top-1 zero-shot test accuracy (%) on ImageNet val set and CelebA dataset respectively. In time complexity analyses, k denotes the number of iterations for unlearning, which we set to 10 in our experiments. K is the number of epochs for training, which is 32. N is the size of whole training set, which is much larger than our sampled forget and retain set N_f and N_r .

Method	FA@1 ↓	FA@5 ↓	TA_IN@1 ↑	TA_CA@1 ↑	Compute Time (\mathcal{O})
Original	73.05	92.22	60.12	61.38	$\mathcal{O}(K \cdot N)$
$1r = 10^{-6}$					
FT [46]	66.08	90.10	60.36	60.70	$\mathcal{O}(k \cdot N_r)$
GA [45]	0.00	0.00	35.88	24.92	$\mathcal{O}(k \cdot N_f)$
GAFT	0.00	0.00	55.52	25.71	$\mathcal{O}(k \cdot (N_f + N_r))$
SalUn [10]	0.00	0.00	55.45	26.11	$\mathcal{O}(N_f) + \mathcal{O}(k \cdot (N_f + N_r))$
$1r = 10^{-7}$					
FT [46]	70.50	92.22	60.26	61.35	$\mathcal{O}(k \cdot N_r)$
GA [45]	0.00	4.91	60.03	53.86	$\mathcal{O}(k \cdot N_f)$
GAFT	2.67	15.89	60.13	55.22	$\mathcal{O}(k \cdot (N_f + N_r))$
SalUn [10]	3.33	15.69	60.26	55.81	$\mathcal{O}(N_f) + \mathcal{O}(k \cdot (N_f + N_r))$
SSD [11]	0.00	0.00	51.84	35.96	$\mathcal{O}(N_f + N_r)$
Ours	0.00	0.00	59.96	58.32	$\mathcal{O}(N_f + N_r)$

Further, we explore the simultaneous unlearning across multiple layers for various tasks in Section 4.5. Additional examples of unlearning, extending beyond identities, are detailed in Section 4.6.

4.3 Unlearning stable diffusion

Stable diffusion models exhibit remarkable capabilities in text comprehension and the generation and manipulation of personal images. For instance, when prompted with "A portrait of Elon Musk," these models can produce a high-fidelity portrait. Moreover, by altering the prompt, one can generate imaginative content, such as a vivid depiction of "Elon Musk on Mars." However, the potential misuse of such powerful tools raises significant concerns regarding the harm they can cause to the data provider. In this study, we demonstrate a method to effectively erase personal information from the image generation model, ensuring that prompts related to the erased individual fail to produce accurate results. As shown in Figure 4, our approach to unlearning Elon Musk interestingly results in representations of electronic circuits, consistently across various prompts, without compromising the model’s general capability to generate a diverse range of other objects. Contrarily, alternative methods not only struggle to accurately render portraits of other individuals but also degrade the image quality of unrelated objects.

In addition to identity removal for privacy protection, we address copyright concerns that increasingly challenge generative models. We successfully apply our method to remove copyright-protected content, specifically targeting well-known characters such as Marvel’s “Iron Man” and Walt Disney’s “Mickey Mouse.” Figure 5 illustrates that our technique precisely unlearns the

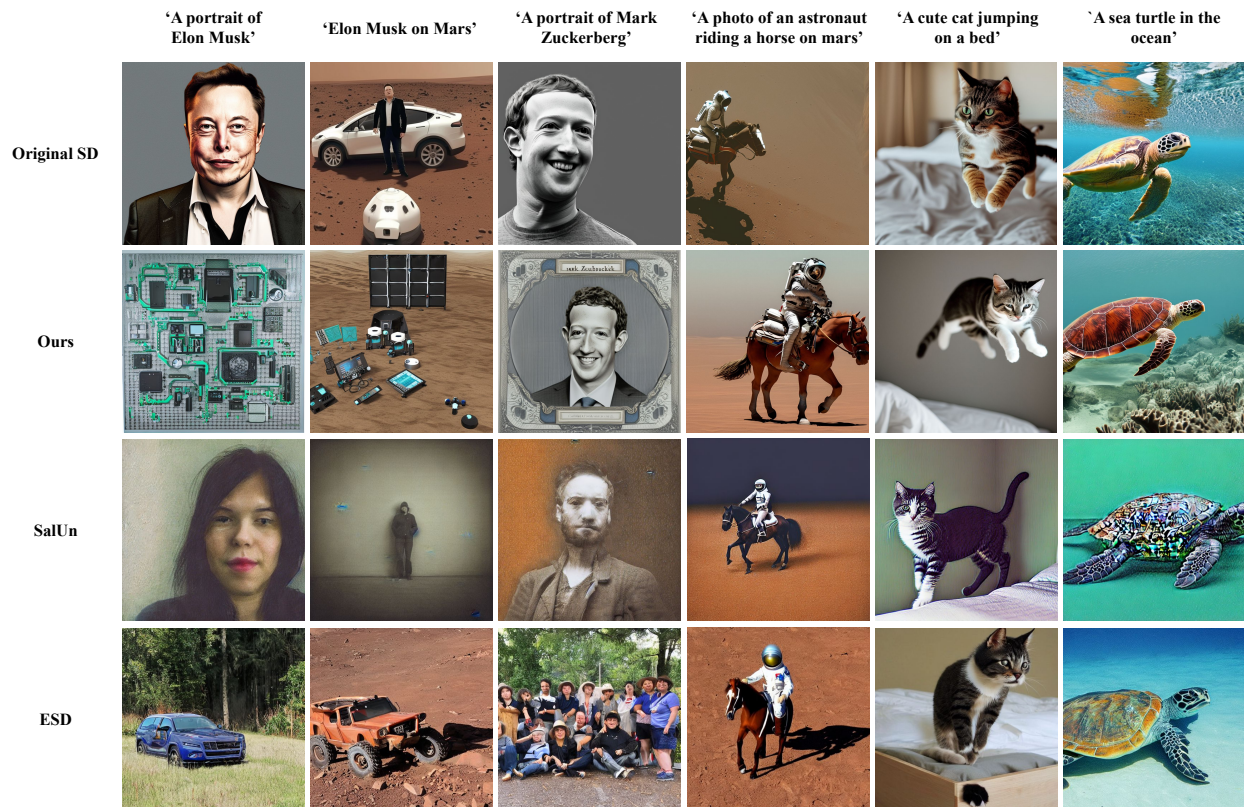


Figure 4: Unlearn performance on stable diffusion. First row shows the generated images from the original pretrained model, the second row shows the output of unlearned model, where Elon Musk is unlearned. We can see that Elon Musk is effectively unlearned, whereas other objects are unaffected. Comparing methods in the bottom two rows suffer from hurting general utility.

targeted concepts, effectively disabling the generation of images associated with these copyrighted entities while preserving the model’s capability to produce images of other concepts. Further examples are detailed in Section D.

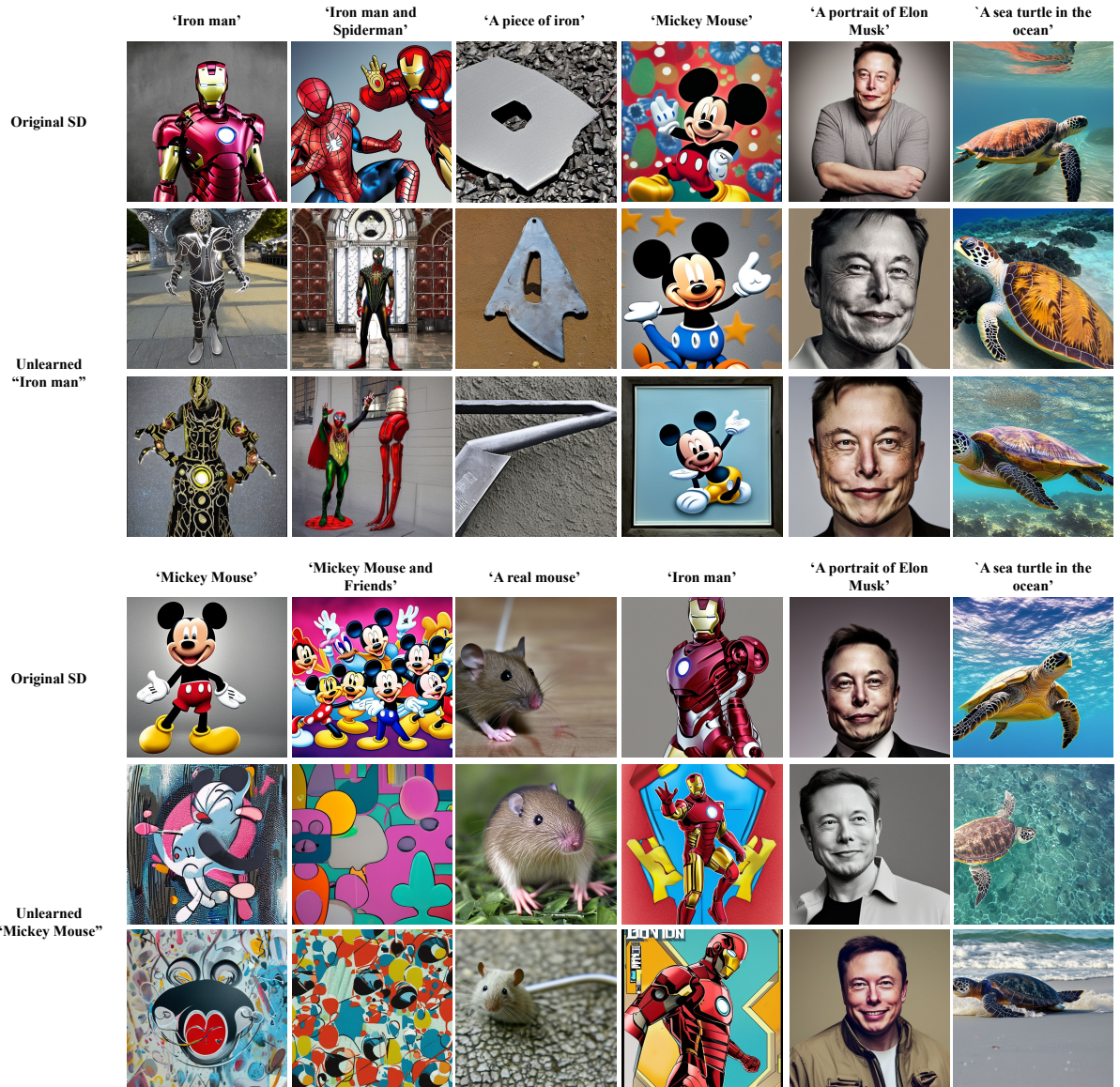


Figure 5: Qualitative evaluation on unlearning copyright characters “Iron man” and “Mickey Mouse” from the Stable Diffusion. Our method precisely unlearned copyright protected concepts from SD, while the image generation quality on other concepts is highly preserved.

4.4 Unlearning VLMs

VLMs demonstrate impressive ability in visual understanding and question answering. For example, when provided with an image of a person, these models can accurately identify and name the individual depicted. Figure 6 demonstrates this by showing that when given an image of Elon Musk and asked, “What’s the name of the person in this image?”, the model correctly identifies him. Our method effectively makes the model “forget” certain subjects; for instance, it erroneously identifies Elon Musk as Michael Jackson. This alteration does not significantly impact the model’s

overall utility. Additional examples of this phenomenon are discussed in Section E.

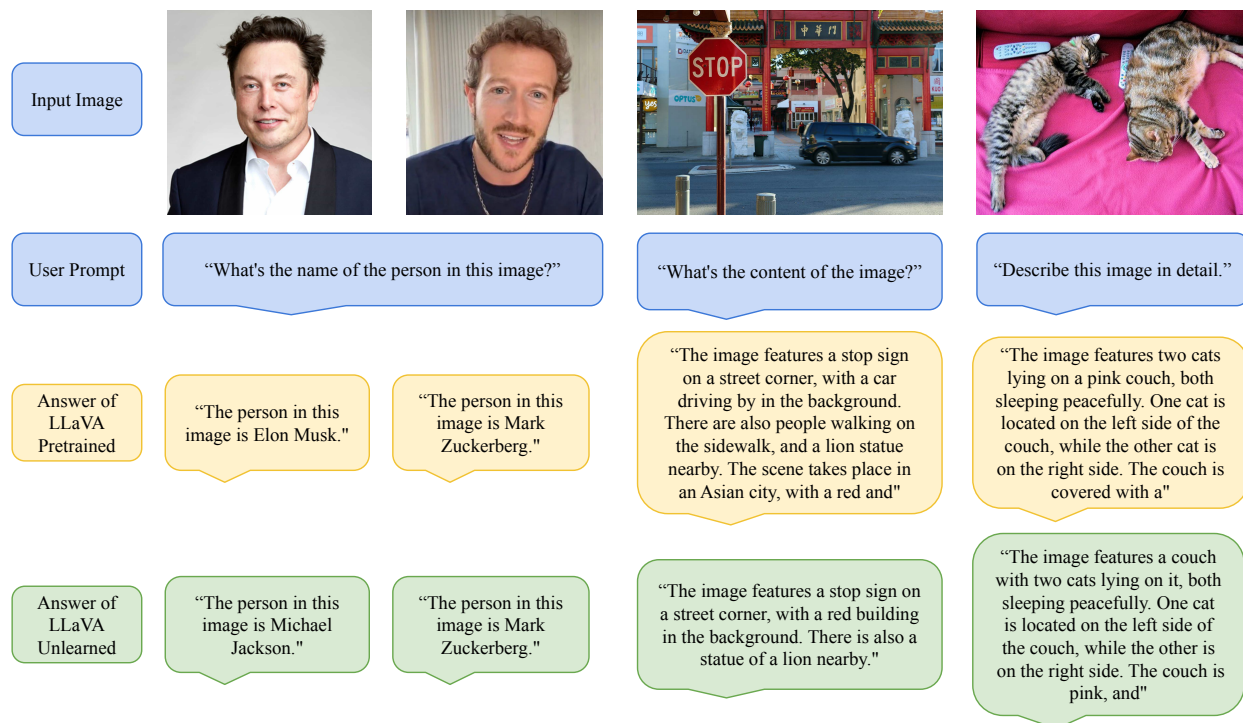
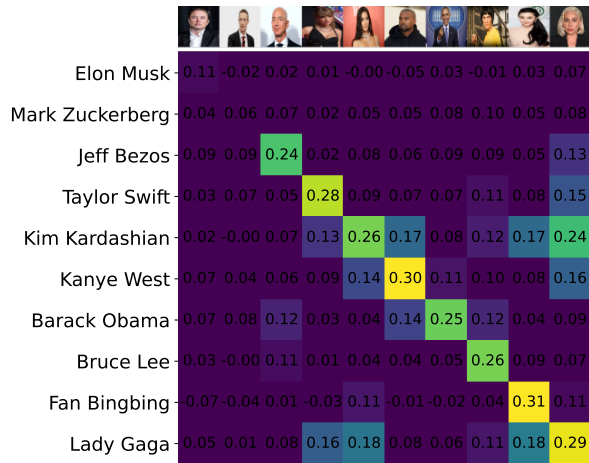


Figure 6: Unlearn performance on LLaVA 1.5. First row shows the generated images from the original pretrained model, the second row shows the output of unlearned model, where Elon Musk is unlearned. We can see that Elon Musk is effectively unlearned, whereas other subjects are unaffected.

4.5 Joint update for unlearning multiple identities

We study the composite effect of our approach where we unlearn multiple tasks simultaneously. For instance, in the task of unlearning multiple identities, we take the gradients calculated for each identity on the original model, and then perform layer updates to simultaneously forget all of them. We demonstrate our results in Figure. 7, where we successfully unlearn (a) {Elon Musk, Mark Zuckerberg} and (b) {Elon Musk, Taylor Swift}.



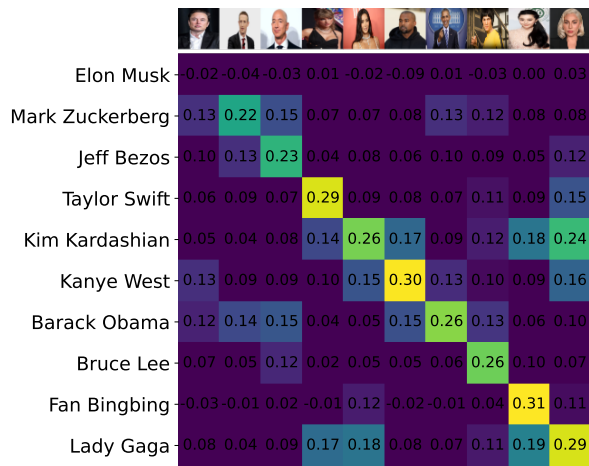
(a) Cosine similarity matrix after unlearning Elon Musk and Mark Zuckerberg



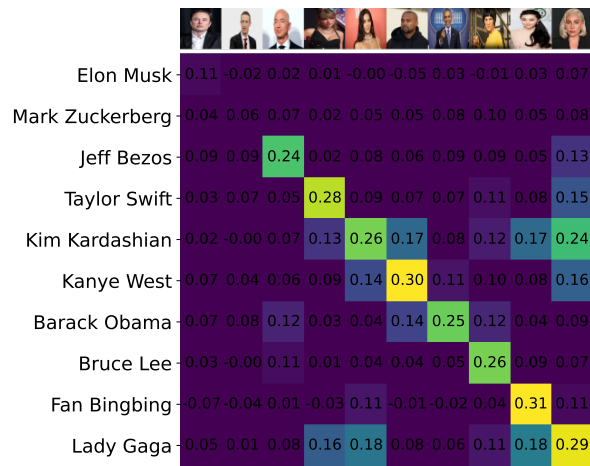
(b) Cosine similarity matrix after unlearning Elon Musk and Taylor Swift

Figure 7: Cosine similarity matrix of image and text pairs after unlearning multiple name identities (see Figure 10a for cosine similarity matrix on original model). After unlearning, the image and text pair of both selected names are not matched, while other persons are only slightly affected. Here the 9th vision attention out projection layer and the 11th vision attention out projection layer are unlearned for Elon Musk and the other identity respectively. CLIP model: ViT-B-32.

Furthermore, we investigate how the unlearning performance varies as the number of identities to be forgotten increases. The cosine similarity matrices presented in Figure 8 demonstrate our effectiveness after identifying different layers associated with different names (see Figure 9), and performing joint updating on different layers.



(a) $N = 1$



(b) $N = 2$



(c) $N = 3$



(d) $N = 4$



(e) $N = 5$



(f) $N = 6$

Figure 8: Cosine similarity matrices after unlearning N identities, where $N \in \{1, 2, \dots, 6\}$.

4.6 Unlearn different concepts

In addition to unlearning personal identities from CLIP, we also sample 7 classes {Basketball, Beach, Castle, Revolver, Rifle, School bus, Sunglasses} from ImageNet to evaluate the unlearning performance of our method on object concepts. For this experiment, we use 10k ImageNet validation images. The results, presented in Table. 2, show the CLIP zero-shot accuracy evaluations for both the forgetting of sampled classes and the retention of other ImageNet classes after unlearning. Our findings indicate that our method effectively reduces the CLIP zero-shot accuracy for the targeted classes to 0.0%, while the accuracy for remaining classes stays high, experiencing only minimal degradation (ranging from 0.03% to 2.03%) compared to the original pre-trained model..

Table 2: Unlearning performance of our method on common object concepts. FA@1 and FA@5 represents the top-1 and top-5 forget accuracy (%) of each class, i.e. zero-shot classification accuracy of unlearned class. FA@1 and FA@5 represents the top-1 and top-5 forget accuracy (%) of all classes of ImageNet. Each row shows the forget class accuracy and average accuracy over all classes of ImageNet before and after unlearning a class. Our method can reduce the accuracy of desired classes to 0.0% while keeping the accuracy of retaining classes close to original model (within 0.06 – 2.03% difference). CLIP model: ViT-B-32.

Forget class	Original				Unlearned			
	FA@1	FA@5	TA@1	TA@5	FA@1 ↓	FA@5 ↓	TA@1 ↑	TA@5 ↑
Basketball	100.0	100.0			0.0	0.0	59.18	84.48
Beach	54.55	72.73			0.0	0.0	59.54	84.78
Castle	87.50	100.0			0.0	0.0	58.13	83.87
Revolver	100.0	100.0	60.16	85.52	0.0	0.0	59.94	85.43
Rifle	42.86	57.14			0.0	0.0	60.08	85.49
School bus	76.92	100.0			0.0	0.0	59.50	89.18
Sunglasses	44.44	55.56			0.0	0.0	60.13	85.23

5 Conclusion

In this study, we introduced a new machine unlearning method characterized by its computational efficiency and efficacy. Our approach, which requires only a single computation of gradients and updates a single layer of the model, not only enhances the feasibility of unlearning large models but also retains the general utility of the models involved. Through rigorous testing on various models, including CLIP, stable diffusion, and VLMs, our method has been shown superior to other state-of-the-art techniques, particularly in its ability to maintain performance on tasks unrelated to the data being unlearned. Moreover, this method’s modular design allows for the simultaneous unlearning of multiple concepts, thereby broadening its applicability and utility in practical scenarios. Future research could expand upon the foundational strategies proposed here to further refine the balance between unlearning effectiveness and utility retention, potentially transforming practices in data privacy and compliance within machine learning.

References

- [1] Regulation (eu) 2016/679 of the european parliament and of the council of 27 april 2016 on the protection of natural persons with regard to the processing of personal data and on the free movement of such data, and repealing directive 95/46/ec (general data protection regulation) (text with eea relevance). *Official Journal of the European Union*, vol. 119, pp. 1–88, 2016. https://eur-lex.europa.eu/legal-content/EN/TXT/?uri=uriserv%3A0J.L_.2016.119.01.0001.01.ENG.
- [2] Evaluation for the neurips machine unlearning competition. August 2023. https://www.kaggle.com/competitions/neurips-2023-machine-unlearning/data?select=Machine_Unlearning_Notion_Metric.pdf.
- [3] Josh Achiam, Steven Adler, Sandhini Agarwal, Lama Ahmad, Ilge Akkaya, Florencia Leoni Aleman, Diogo Almeida, Janko Altenschmidt, Sam Altman, Shyamal Anadkat, et al. Gpt-4 technical report. *arXiv preprint arXiv:2303.08774*, 2023. <https://arxiv.org/abs/2303.08774>.
- [4] Tom Brown, Benjamin Mann, Nick Ryder, Melanie Subbiah, Jared D Kaplan, Prafulla Dhariwal, Arvind Neelakantan, Pranav Shyam, Girish Sastry, Amanda Askell, et al. Language models are few-shot learners. *Advances in neural information processing systems*, 33:1877–1901, 2020. <https://arxiv.org/abs/2005.14165>.
- [5] Yinzhi Cao and Junfeng Yang. Towards making systems forget with machine unlearning. In *2015 IEEE symposium on security and privacy*, pages 463–480. IEEE, 2015. <https://ieeexplore.ieee.org/document/7163042>.
- [6] Mehdi Cherti, Romain Beaumont, Ross Wightman, Mitchell Wortsman, Gabriel Ilharco, Cade Gordon, Christoph Schuhmann, Ludwig Schmidt, and Jenia Jitsev. Reproducible scaling laws for contrastive language-image learning. In *Proceedings of the IEEE/CVF Conference on Computer Vision and Pattern Recognition*, pages 2818–2829, 2023. <https://arxiv.org/abs/2212.07143>.
- [7] Eli Chien, Chao Pan, and Olgica Milenkovic. Certified graph unlearning. *arXiv preprint arXiv:2206.09140*, 2022. <https://arxiv.org/abs/2206.09140>.
- [8] Sumit Chopra, Raia Hadsell, and Yann LeCun. Learning a similarity metric discriminatively, with application to face verification. In *2005 IEEE computer society conference on computer vision and pattern recognition (CVPR'05)*, volume 1, pages 539–546. IEEE, 2005. <https://ieeexplore.ieee.org/document/1467314>.
- [9] Vikram S Chundawat, Ayush K Tarun, Murari Mandal, and Mohan Kankanhalli. Can bad teaching induce forgetting? unlearning in deep networks using an incompetent teacher. In *Proceedings of the AAAI Conference on Artificial Intelligence*, volume 37, pages 7210–7217, 2023. <https://arxiv.org/abs/2205.08096>.
- [10] Chongyu Fan, Jiancheng Liu, Yihua Zhang, Dennis Wei, Eric Wong, and Sijia Liu. Salun: Empowering machine unlearning via gradient-based weight saliency in both image classification and generation. *ICLR*, 2024. <https://arxiv.org/abs/2310.12508>.

- [11] Jack Foster, Stefan Schoepf, and Alexandra Brintrup. Fast machine unlearning without retraining through selective synaptic dampening. In *Proceedings of the AAAI Conference on Artificial Intelligence*, volume 38, pages 12043–12051, 2024. <https://arxiv.org/abs/2308.07707>.
- [12] Rohit Gandikota, Joanna Materzynska, Jaden Fiotto-Kaufman, and David Bau. Erasing concepts from diffusion models. In *Proceedings of the IEEE/CVF International Conference on Computer Vision*, pages 2426–2436, 2023.
- [13] Amin Ghiasi, Hamid Kazemi, Eitan Borgnia, Steven Reich, Manli Shu, Micah Goldblum, Andrew Gordon Wilson, and Tom Goldstein. What do vision transformers learn? a visual exploration. *arXiv preprint arXiv:2212.06727*, 2022. <https://arxiv.org/abs/2212.06727>.
- [14] Shashwat Goel, Ameya Prabhu, Amartya Sanyal, Ser-Nam Lim, Philip Torr, and Ponnurangam Kumaraguru. Towards adversarial evaluations for inexact machine unlearning. *arXiv preprint arXiv:2201.06640*, 2022. <https://arxiv.org/abs/2201.06640>.
- [15] Aditya Golatkar, Alessandro Achille, and Stefano Soatto. Eternal sunshine of the spotless net: Selective forgetting in deep networks. In *Proceedings of the IEEE/CVF Conference on Computer Vision and Pattern Recognition*, pages 9304–9312, 2020. <https://arxiv.org/abs/1911.04933>.
- [16] Aditya Golatkar, Alessandro Achille, and Stefano Soatto. Forgetting outside the box: Scrubbing deep networks of information accessible from input-output observations. In *Computer Vision—ECCV 2020: 16th European Conference, Glasgow, UK, August 23–28, 2020, Proceedings, Part XXIX 16*, pages 383–398. Springer, 2020. <https://arxiv.org/abs/2003.02960>.
- [17] Chuan Guo, Tom Goldstein, Awni Hannun, and Laurens Van Der Maaten. Certified data removal from machine learning models. *ICML*, 2020. <https://arxiv.org/abs/1911.03030>.
- [18] Babak Hassibi, David G Stork, and Gregory J Wolff. Optimal brain surgeon and general network pruning. In *IEEE international conference on neural networks*, pages 293–299. IEEE, 1993. <https://ieeexplore.ieee.org/document/298572>.
- [19] Jinghan Jia, Jiancheng Liu, Parikshit Ram, Yuguang Yao, Gaowen Liu, Yang Liu, Pranay Sharma, and Sijia Liu. Model sparsification can simplify machine unlearning. *NeurIPS*, 2023. <https://arxiv.org/abs/2304.04934>.
- [20] Jared Kaplan, Sam McCandlish, Tom Henighan, Tom B Brown, Benjamin Chess, Rewon Child, Scott Gray, Alec Radford, Jeffrey Wu, and Dario Amodei. Scaling laws for neural language models. *arXiv preprint arXiv:2001.08361*, 2020. <https://arxiv.org/abs/2001.08361>.
- [21] Steven M Kay. *Fundamentals of statistical signal processing: estimation theory*. Prentice-Hall, Inc., 1993. <https://dl.acm.org/doi/abs/10.5555/151045>.
- [22] James Kirkpatrick, Razvan Pascanu, Neil Rabinowitz, Joel Veness, Guillaume Desjardins, Andrei A Rusu, Kieran Milan, John Quan, Tiago Ramalho, Agnieszka Grabska-Barwinska, et al. Overcoming catastrophic forgetting in neural networks. *Proceedings of the national academy of sciences*, 114(13):3521–3526, 2017. <https://arxiv.org/abs/1612.00796>.

- [23] Meghdad Kurmanji, Peter Triantafillou, and Eleni Triantafillou. Towards unbounded machine unlearning. *arXiv preprint arXiv:2302.09880*, 2023. <https://arxiv.org/abs/2302.09880>.
- [24] Christoph Leiter, Ran Zhang, Yanran Chen, Jonas Belouadi, Daniil Larionov, Vivian Fresen, and Steffen Eger. Chatgpt: A meta-analysis after 2.5 months. *Machine Learning with Applications*, 16:100541, 2024. <https://arxiv.org/abs/2302.13795>.
- [25] Guihong Li, Hsiang Hsu, Radu Marculescu, et al. Machine unlearning for image-to-image generative models. *ICLR*, 2024. <https://arxiv.org/abs/2402.00351>.
- [26] Yanwei Li, Yuechen Zhang, Chengyao Wang, Zhisheng Zhong, Yixin Chen, Ruihang Chu, Shaoteng Liu, and Jiaya Jia. Mini-gemini: Mining the potential of multi-modality vision language models. *arXiv preprint arXiv:2403.18814*, 2024. <https://arxiv.org/abs/2403.18814>.
- [27] Haotian Liu, Chunyuan Li, Yuheng Li, and Yong Jae Lee. Improved baselines with visual instruction tuning. *arXiv preprint arXiv:2310.03744*, 2023. <https://arxiv.org/abs/2310.03744>.
- [28] Haotian Liu, Chunyuan Li, Qingyang Wu, and Yong Jae Lee. Visual instruction tuning. *Advances in neural information processing systems*, 36, 2024. <https://arxiv.org/abs/2304.08485>.
- [29] Sijia Liu, Yuanshun Yao, Jinghan Jia, Stephen Casper, Nathalie Baracaldo, Peter Hase, Xiaojun Xu, Yuguang Yao, Hang Li, Kush R Varshney, et al. Rethinking machine unlearning for large language models. *arXiv preprint arXiv:2402.08787*, 2024. <https://arxiv.org/abs/2402.08787>.
- [30] Ziwei Liu, Ping Luo, Xiaogang Wang, and Xiaoou Tang. Deep learning face attributes in the wild. In *Proceedings of the IEEE international conference on computer vision*, pages 3730–3738, 2015. <https://arxiv.org/abs/1411.7766>.
- [31] R Timothy Marler and Jasbir S Arora. The weighted sum method for multi-objective optimization: new insights. *Structural and multidisciplinary optimization*, 41:853–862, 2010. <https://link.springer.com/article/10.1007/s00158-009-0460-7>.
- [32] Thanh Tam Nguyen, Thanh Trung Huynh, Phi Le Nguyen, Alan Wee-Chung Liew, Hongzhi Yin, and Quoc Viet Hung Nguyen. A survey of machine unlearning. *arXiv preprint arXiv:2209.02299*, 2022. <https://arxiv.org/abs/2209.02299>.
- [33] Alex Nichol, Prafulla Dhariwal, Aditya Ramesh, Pranav Shyam, Pamela Mishkin, Bob McGrew, Ilya Sutskever, and Mark Chen. Glide: Towards photorealistic image generation and editing with text-guided diffusion models. *ICML*, 2022. <https://arxiv.org/abs/2112.10741>.
- [34] Chris Olah, Alexander Mordvintsev, and Ludwig Schubert. Feature visualization. *Distill*, 2(11):e7, 2017. <https://distill.pub/2017/feature-visualization/>.
- [35] Dustin Podell, Zion English, Kyle Lacey, Andreas Blattmann, Tim Dockhorn, Jonas Müller, Joe Penna, and Robin Rombach. Sd-xl: Improving latent diffusion models for high-resolution image synthesis. *arXiv preprint arXiv:2307.01952*, 2023. <https://arxiv.org/abs/2307.01952>.

- [36] Alec Radford, Jong Wook Kim, Chris Hallacy, Aditya Ramesh, Gabriel Goh, Sandhini Agarwal, Girish Sastry, Amanda Askell, Pamela Mishkin, Jack Clark, et al. Learning transferable visual models from natural language supervision. In *International conference on machine learning*, pages 8748–8763. PMLR, 2021. <https://arxiv.org/abs/2103.00020>.
- [37] Alec Radford, Karthik Narasimhan, Tim Salimans, Ilya Sutskever, et al. Improving language understanding by generative pre-training. 2018. <https://openai.com/index/language-unsupervised/>.
- [38] Alec Radford, Jeffrey Wu, Rewon Child, David Luan, Dario Amodei, Ilya Sutskever, et al. Language models are unsupervised multitask learners. *OpenAI blog*, 1(8):9, 2019. <https://openai.com/index/better-language-models/>.
- [39] Robin Rombach, Andreas Blattmann, Dominik Lorenz, Patrick Esser, and Björn Ommer. High-resolution image synthesis with latent diffusion models. In *Proceedings of the IEEE/CVF conference on computer vision and pattern recognition*, pages 10684–10695, 2022. <https://arxiv.org/abs/2112.10752>.
- [40] Tim Salimans and Jonathan Ho. Progressive distillation for fast sampling of diffusion models. *ICLR*, 2022. <https://arxiv.org/abs/2202.00512>.
- [41] Christoph Schuhmann, Romain Beaumont, Richard Vencu, Cade Gordon, Ross Wightman, Mehdi Cherti, Theo Coombes, Aarush Katta, Clayton Mullis, Mitchell Wortsman, et al. Laion-5b: An open large-scale dataset for training next generation image-text models. *Advances in Neural Information Processing Systems*, 35:25278–25294, 2022. <https://arxiv.org/abs/2210.08402>.
- [42] Christoph Schuhmann, Richard Vencu, Romain Beaumont, Robert Kaczmarczyk, Clayton Mullis, Aarush Katta, Theo Coombes, Jenia Jitsev, and Aran Komatsuzaki. Laion-400m: Open dataset of clip-filtered 400 million image-text pairs. *arXiv preprint arXiv:2111.02114*, 2021. <https://arxiv.org/abs/2111.02114>.
- [43] Thanveer Shaik, Xiaohui Tao, Haoran Xie, Lin Li, Xiaofeng Zhu, and Qing Li. Exploring the landscape of machine unlearning: A survey and taxonomy. *arXiv preprint arXiv:2305.06360*, 2023. <https://arxiv.org/abs/2305.06360>.
- [44] David Thiel. Identifying and eliminating csam in generative ml training data and models. Technical report, Technical report, Stanford University, Palo Alto, CA, 2023. URL <https://purl.stanford.edu/kh752sm9123>, 2023.
- [45] Anvith Thudi, Gabriel Deza, Varun Chandrasekaran, and Nicolas Papernot. Unrolling sgd: Understanding factors influencing machine unlearning. In *2022 IEEE 7th European Symposium on Security and Privacy (EuroS&P)*, pages 303–319. IEEE, 2022. <https://arxiv.org/abs/2109.13398>.
- [46] Alexander Warnecke, Lukas Pirch, Christian Wressnegger, and Konrad Rieck. Machine unlearning of features and labels. *Network and Distributed System Security Symposium (NDSS)*, 2023. <https://arxiv.org/abs/2108.11577>.

- [47] Ling Yang, Zhilong Zhang, Yang Song, Shenda Hong, Runsheng Xu, Yue Zhao, Wentao Zhang, Bin Cui, and Ming-Hsuan Yang. Diffusion models: A comprehensive survey of methods and applications. *ACM Computing Surveys*, 56(4):1–39, 2023. <https://arxiv.org/abs/2209.00796>.
- [48] Yuanshun Yao, Xiaojun Xu, and Yang Liu. Large language model unlearning. *ICLR*, 2024. <https://arxiv.org/pdf/2310.10683>.
- [49] Matthew D Zeiler and Rob Fergus. Visualizing and understanding convolutional networks. In *Computer Vision—ECCV 2014: 13th European Conference, Zurich, Switzerland, September 6–12, 2014, Proceedings, Part I 13*, pages 818–833. Springer, 2014. <https://arxiv.org/abs/1311.2901>.
- [50] Jingyi Zhang, Jiaxing Huang, Sheng Jin, and Shijian Lu. Vision-language models for vision tasks: A survey. *IEEE Transactions on Pattern Analysis and Machine Intelligence*, 2024. <https://arxiv.org/abs/2304.00685>.

A More named identities

In addition to the experiment of unlearning name “Elon Musk” from CLIP model discussed in Sec. 4.2 of the main text, we have expanded our study to include a broader set of identities: {Kanye West, Barack Obama, Bruce Lee, Fan Bingbing, Lady Gaga}. These names were selected from the CelebA dataset to represent a diverse cross-section of ethnicities and genders. Our methodology effectively pinpointed the crucial layers associated with each name. These layers can then be specifically targeted to efficiently unlearn the corresponding identity from the CLIP model.

Figure 9 illustrates the Pareto-front plots that identify important layers selected by our method for unlearning various name identities. Furthermore, as demonstrated in Figure 10, our approach successfully removed the desired names from the CLIP model.

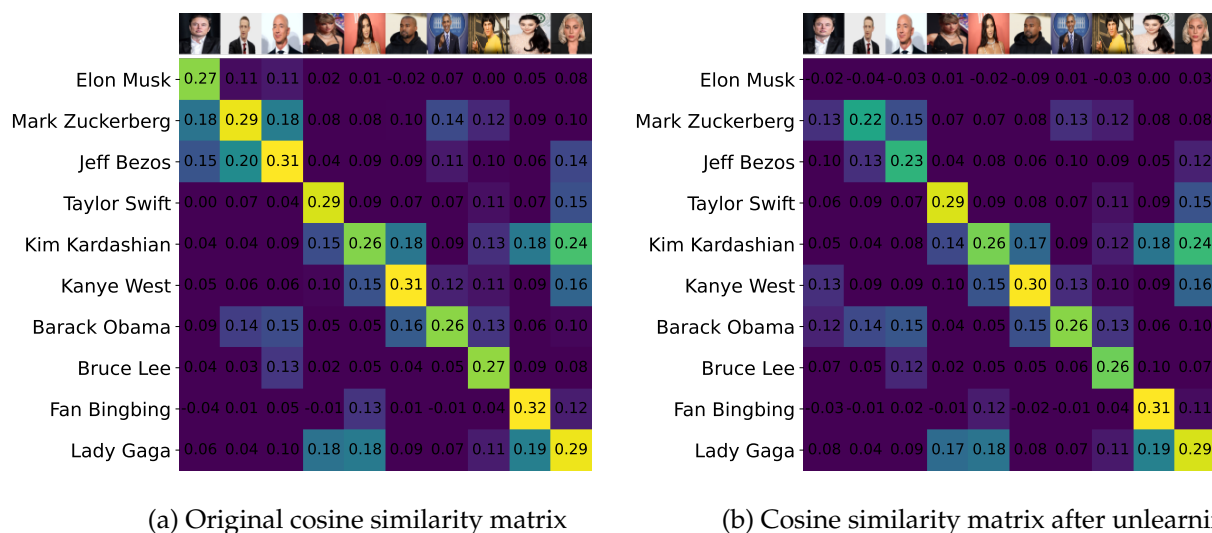
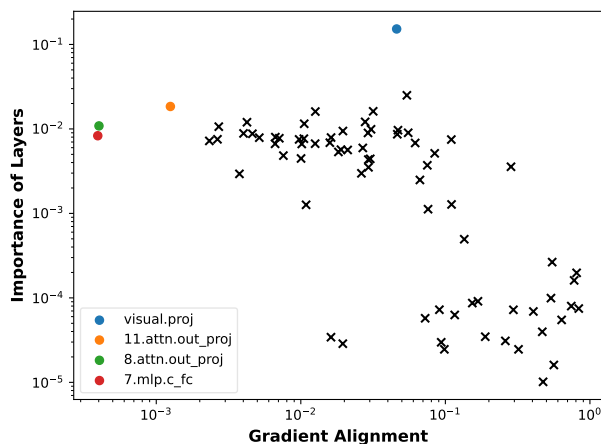


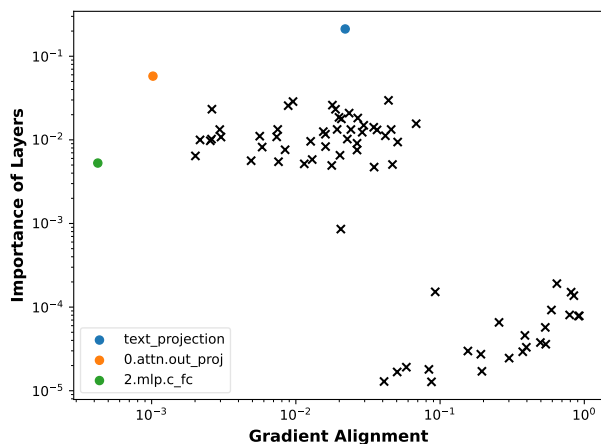
Figure 10: Cosine similarity matrix of image and text pairs before and after unlearning Elon Musk. After unlearning, the image and text pair of Elon Musk are not matched, while other persons are only slightly affected. Here the vision attention out projection layer at the 9th resblock is unlearned. CLIP model: ViT-B-16

B More CLIP models

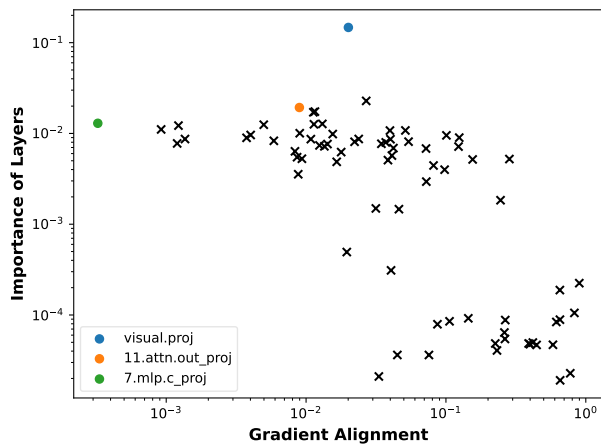
Here we show experiments using an expanded set of model architectures: {ViT-B-16, ViT-L-14, EVA01-g-14}. As illustrated in Figure 13, our method demonstrates scalability and effectiveness across a range of model sizes, from 149.62 million parameters (ViT-B-16) to 1.136 billion parameters (EVA01-g-14). This underscores the flexibility of our approach to accommodate models of different scales.



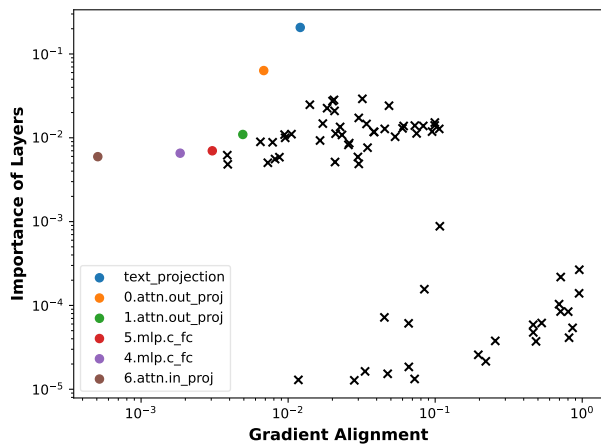
(a) Vision layer Pareto - Mark Zuckerberg



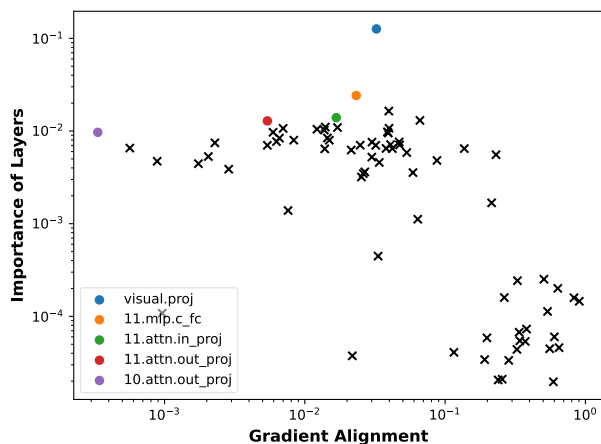
(b) Language layer Pareto - Mark Zuckerberg



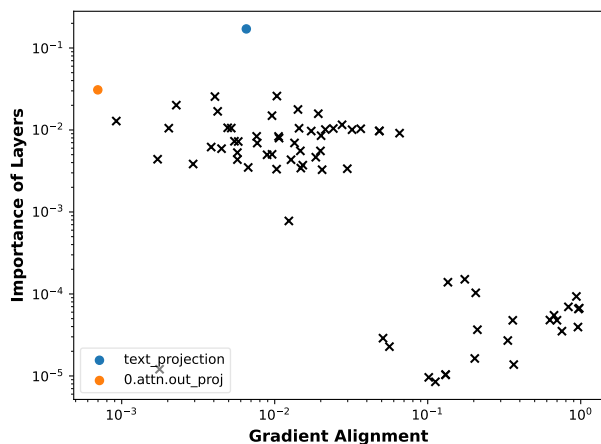
(c) Vision layer Pareto - Jeff Bezos



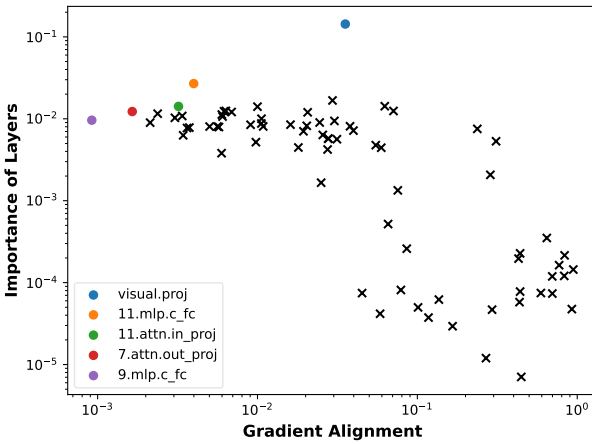
(d) Language layer Pareto - Jeff Bezos



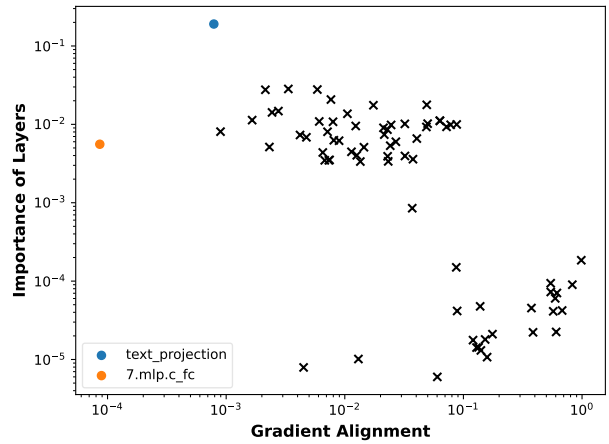
(e) Vision layer Pareto - Taylor Swift



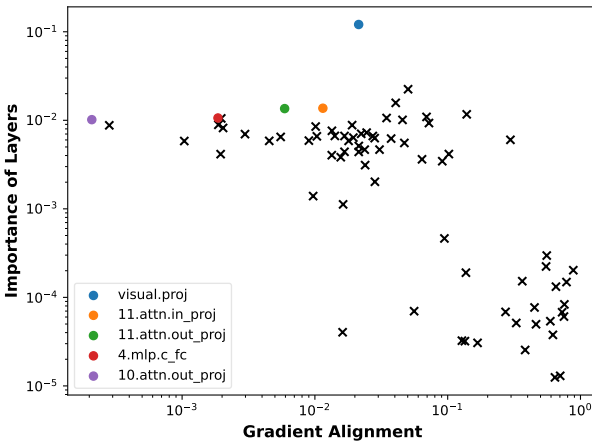
(f) Language layer Pareto - Taylor Swift



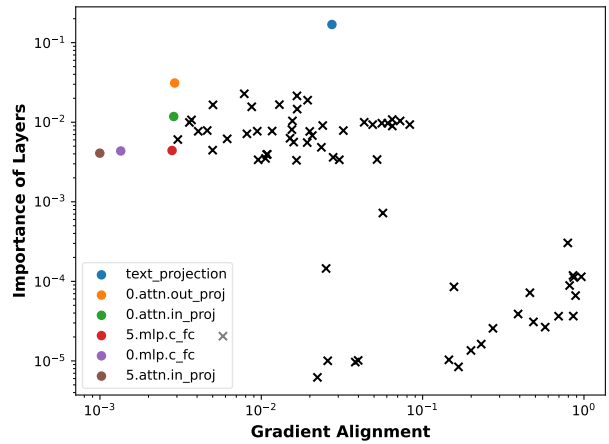
(g) Vision layer Pareto - Kim Kardashian



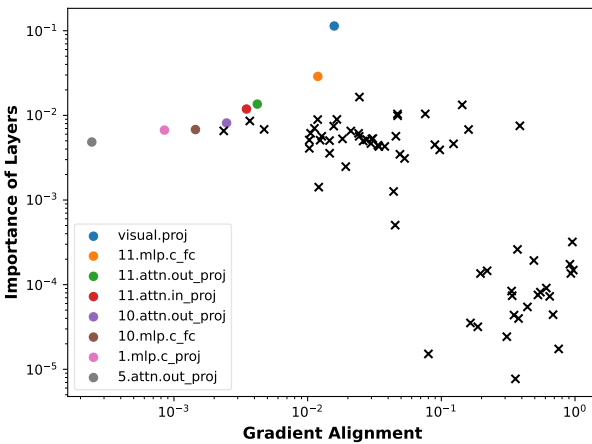
(h) Language layer Pareto - Kim Kardashian



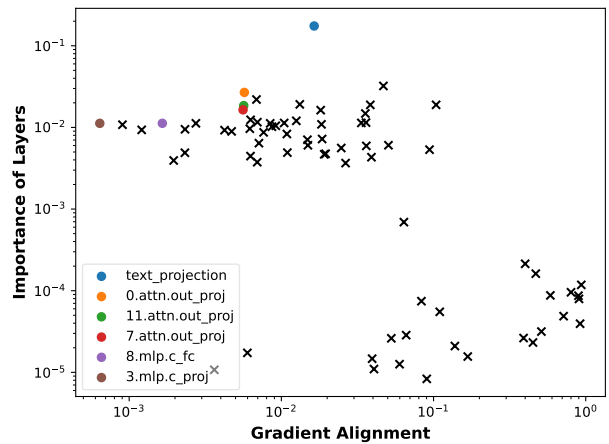
(i) Vision layer Pareto - Kanye West



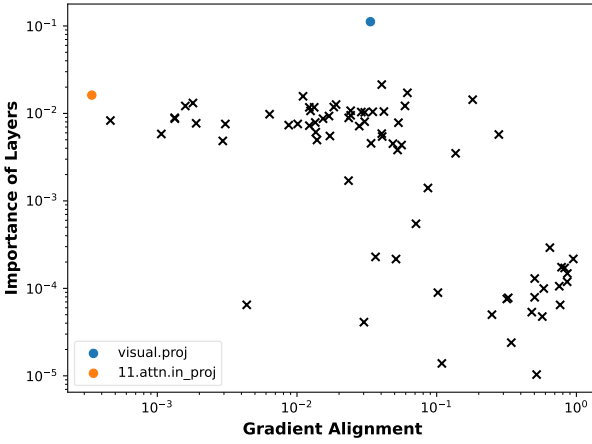
(j) Language layer Pareto - Kanye West



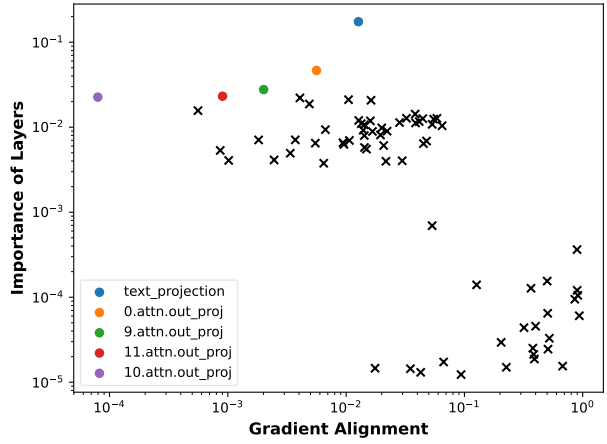
(k) Vision layer Pareto - Barack Obama



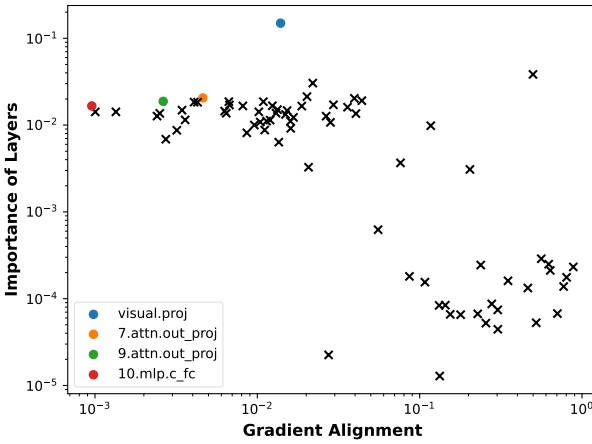
(l) Language layer Pareto - Barack Obama



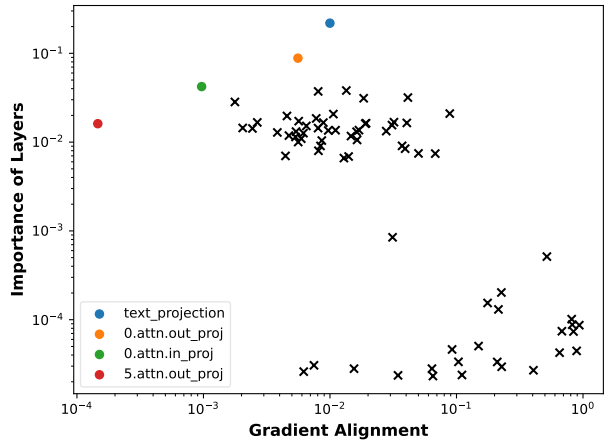
(m) Vision layer Pareto - Bruce Lee



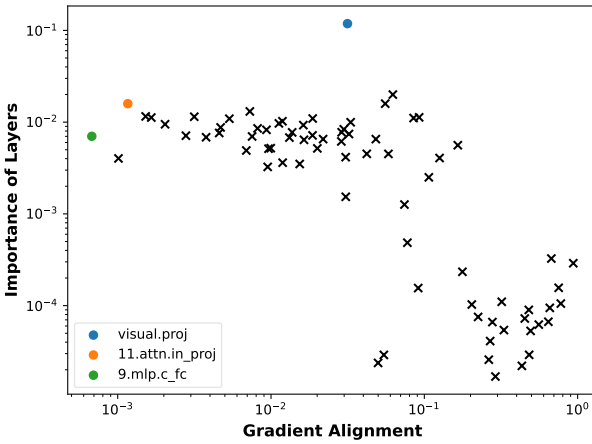
(n) Language layer Pareto - Bruce Lee



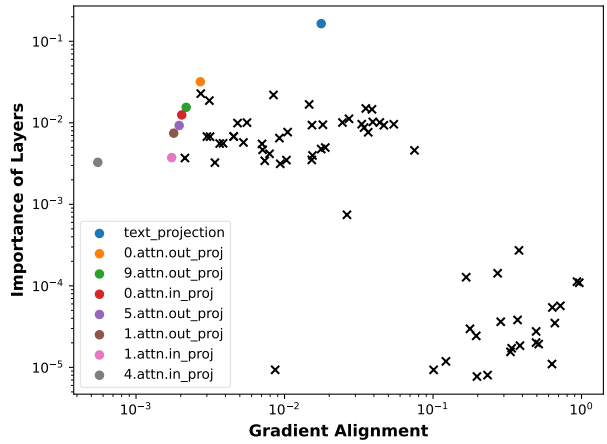
(o) Vision layer Pareto - Fan Bingbing



(p) Language layer Pareto - Fan Bingbing

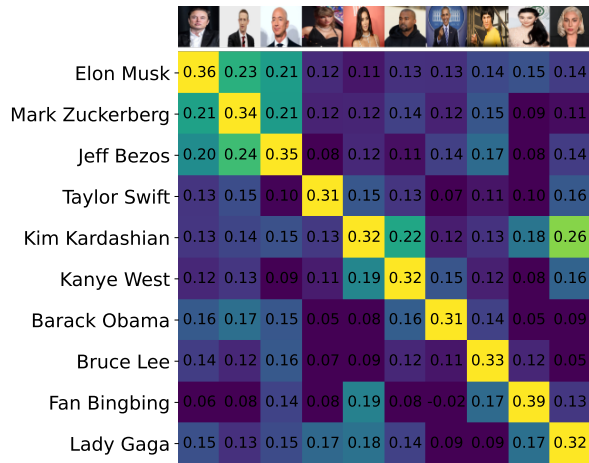


(q) Vision layer Pareto - Lady Gaga

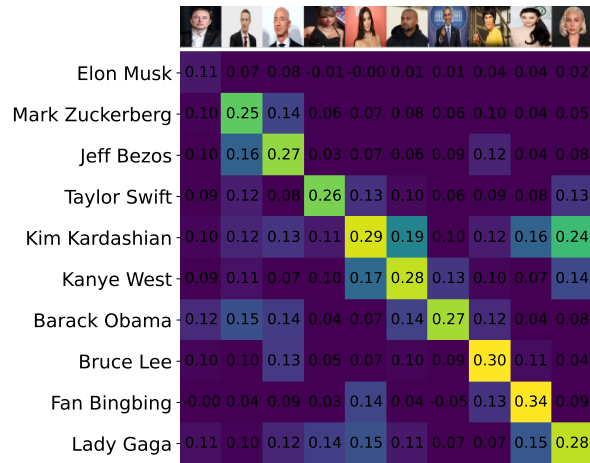


(r) Language layer Pareto - Lady Gaga

Figure 9: More identities, in addition to Figure 2. CLIP variant: ViT-B-32

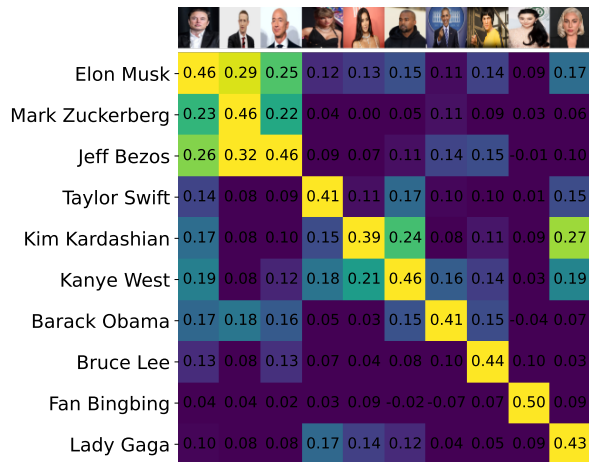


(a) Original cosine similarity matrix



(b) Cosine similarity matrix after unlearning

Figure 11: Cosine similarity matrix of image and text pairs before and after unlearning Elon Musk. After unlearning, the image and text pair of Elon Musk are not matched, while other persons are only slightly affected. Here the vision projection layer within the MLP of the 23rd resblock is unlearned. CLIP variant: ViT-L-14

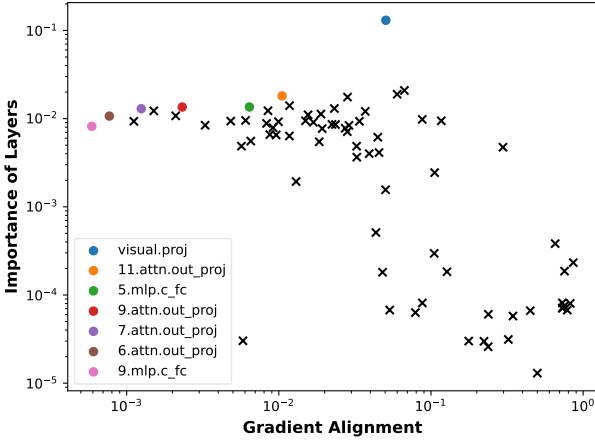


(a) Original cosine similarity matrix

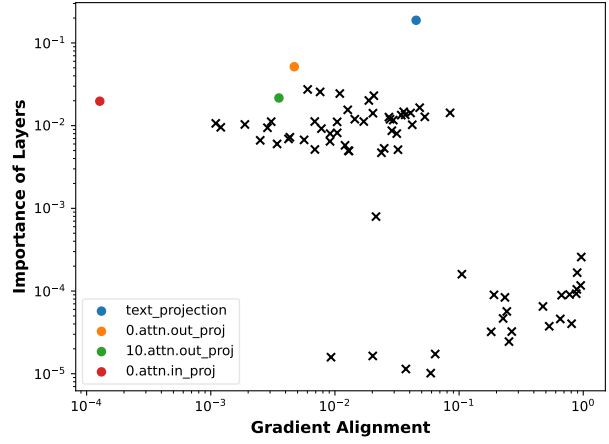


(b) Cosine similarity matrix after unlearning

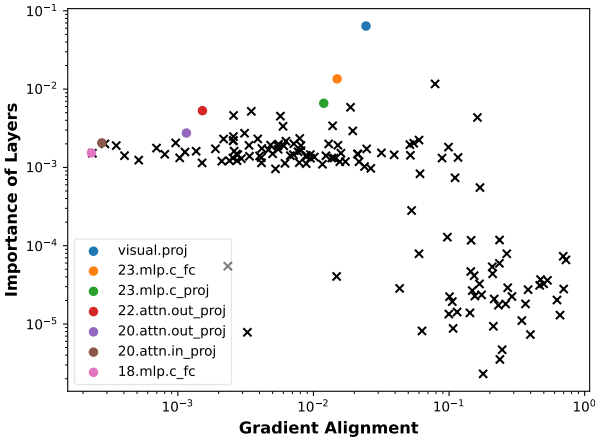
Figure 12: Cosine similarity matrix of image and text pairs before and after unlearning Elon Musk. After unlearning, the image and text pair of Elon Musk are not matched, while other persons are only affected. Here the language attention out projection layer at the 11th resblock is unlearned. CLIP model: EVA01-g-14.



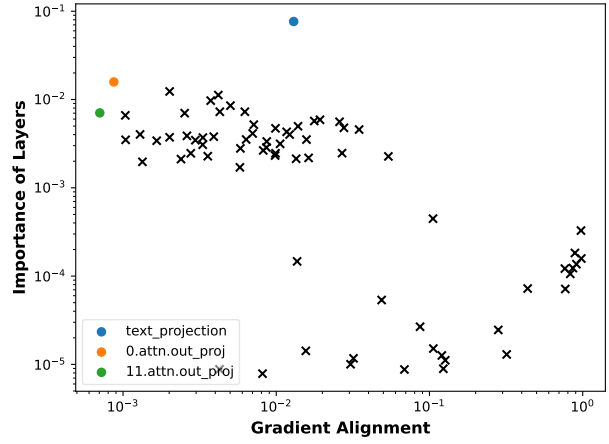
(a) Vision layer Pareto - ViT-B-16



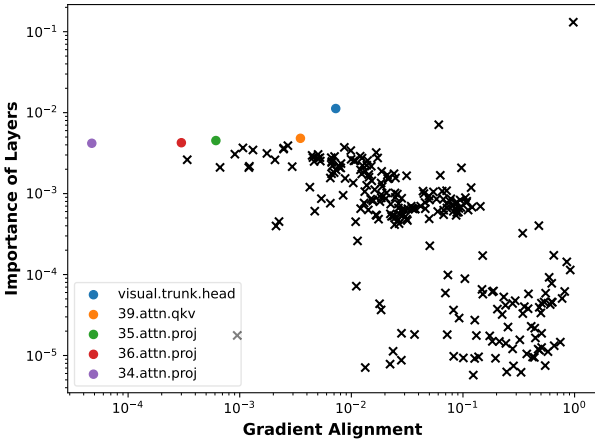
(b) Language layer Pareto - ViT-B-16



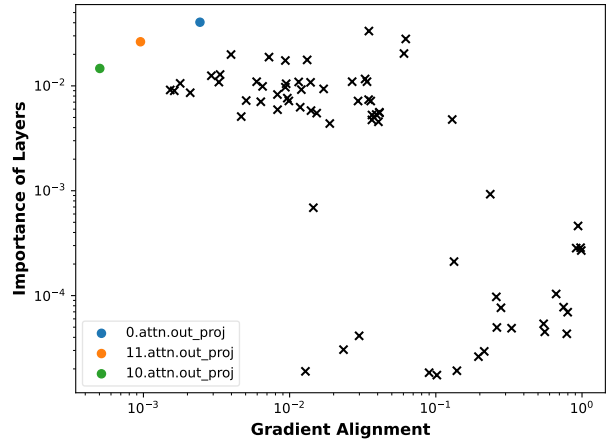
(c) Vision layer Pareto - ViT-L-14



(d) Language layer Pareto - ViT-L-14



(e) Vision layer Pareto - EVA01-g-14

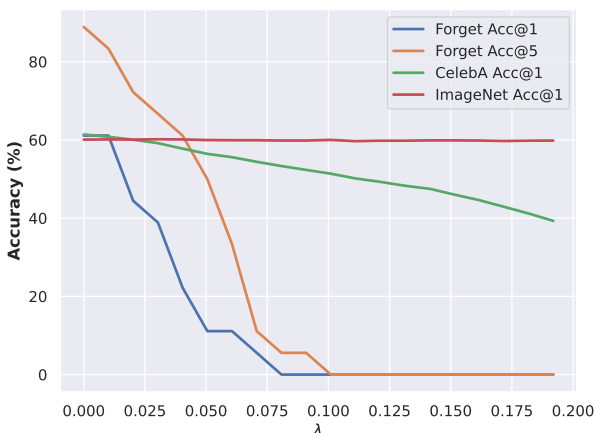


(f) Language layer Pareto - EVA01-g-14

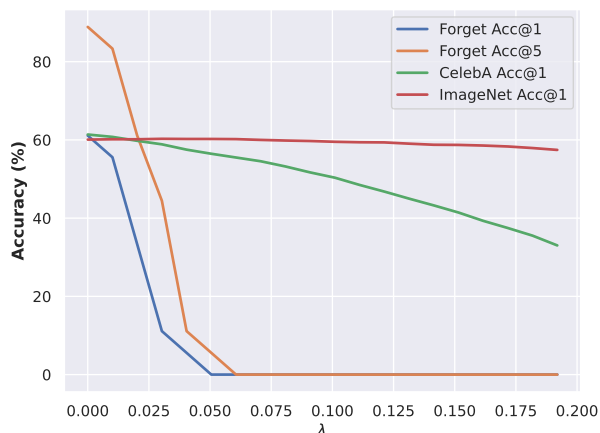
Figure 13: More CLIP models, in addition to Sec 4.2. Unlearning name Elon Musk from CLIP variant: {ViT-B-16, ViT-L-14, and EVA01-g-14}

C Linearity of unlearning trajectory of different layers

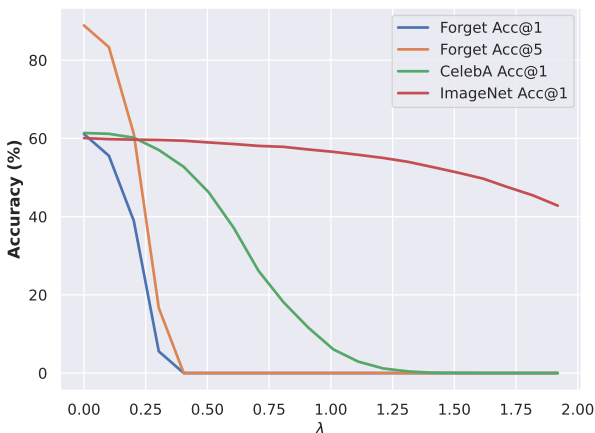
In addition to the layers presented in Figure 2 (c) and (d), we show in Figure 14 that different layers show similar monotonic behaviors however their utility performance may vary, thus it is important to select the best layer from the pareto set for best performance.



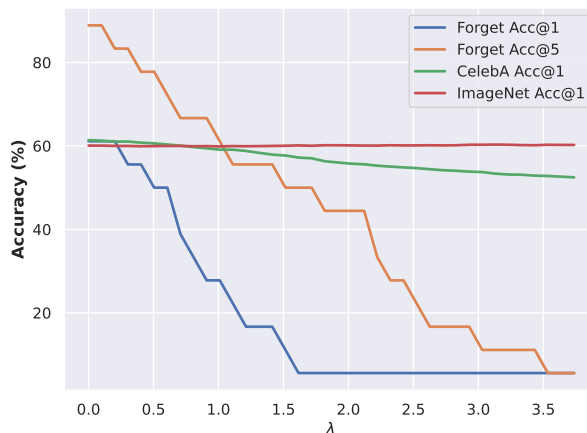
(a) Vision layer `visual.proj`



(b) Language layer `text_projection`



(c) Vision layer `11.mlp.c_fc`



(d) Language layer `11.attn.in_proj`

Figure 14: More examples of unlearning different layers. Correspond to Figure 2. The performance changes monotonically with the step size λ .

D More examples on SD

To demonstrate the performance and practical utility of our method, we further consider unlearning more celebrity names and more scenarios including unlearning copyright characters and novel concepts from Stable Diffusion.

More celebrity name. Beyond unlearning “Elon Musk” from Stable Diffusion, which is presented in the Figure 4, here we also provide additional qualitative evaluations on unlearning other celebrity

names {Taylor Swift, Jeff Bezos} with our method in Figure 15.

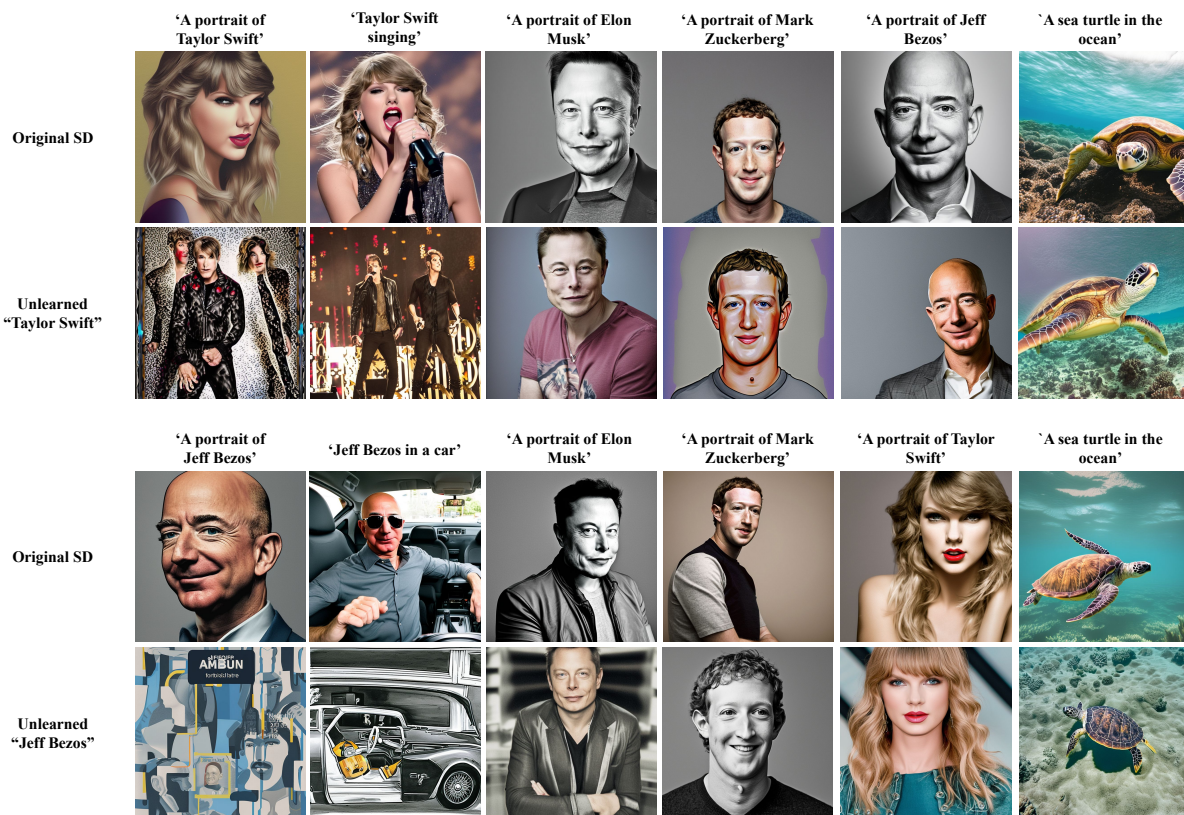


Figure 15: Qualitative evaluation on unlearning celebrity names Taylor Swift and Jeff Bezos from the Stable Diffusion.

Novel concept. One of the intriguing properties of the Stable Diffusion is its ability to generalize image generation to novel concepts that are infrequently or never observed in the real world. In this experiment, we explore the unlearning of a unique concept, "Avocado chair" from Stable Diffusion. We first generate 500 image using SD with the prompt "An avocado chair" to create the forget set. In Figure 16, we show that our method successfully unlearn the concept "Avocado chair" from SD, resulting in the model's inability to generate images corresponding to this specific concept.

However, it is noteworthy that the model's capability to generate images related to the constituent atomic concepts—namely "Avocado" and "Chair"—is also compromised. We hypothesize that this occurs due to the model's treatment of novel concepts as compositions of atomic concepts. For example, the concept "Avocado chair" is interpreted by the model as "Avocado" plus "Chair." Consequently, when a novel concept is unlearned, the associated atomic concepts are inadvertently affected as well. This highlights a challenge in the model's approach to handling the interoperability of novel and atomic concepts.

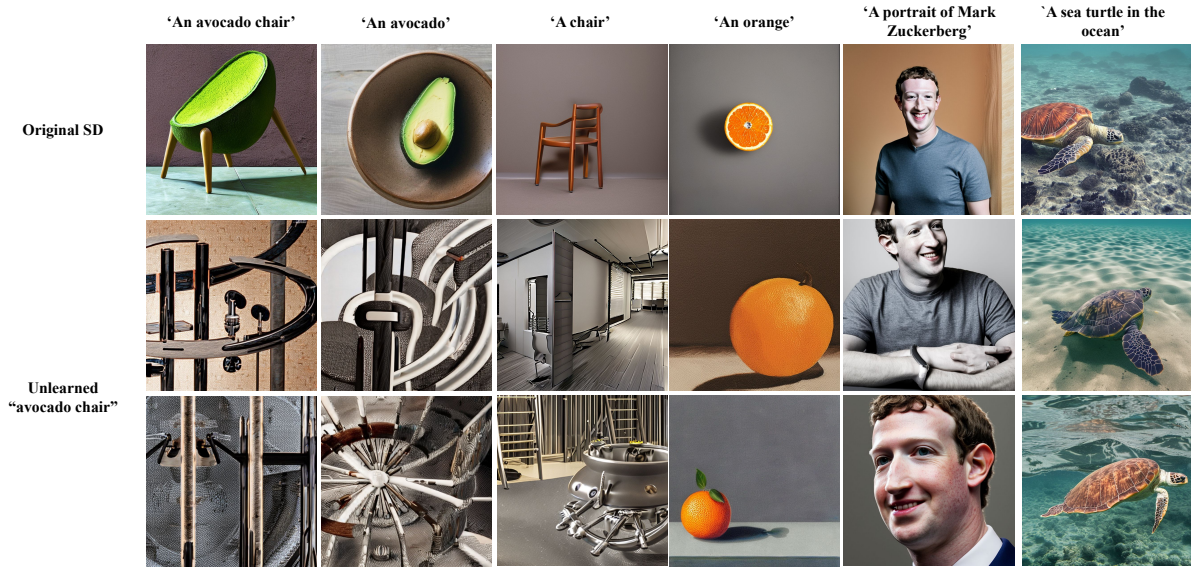


Figure 16: Qualitative evaluation on unlearning a novel concept “Avocado chair” from the Stable Diffusion.

E More examples on VLM

In addition to results presented in the main text Figure 6, we also present additional results on unlearning a different name “Taylor Swift” from VLM in Figure 17. We demonstrate that our method can anonymizes celebrity names from the pretrained Vision-language models, and simultaneously preserves the model’s ability on image understanding, reasoning and distribution shift robustness on art work, cartoon style images.

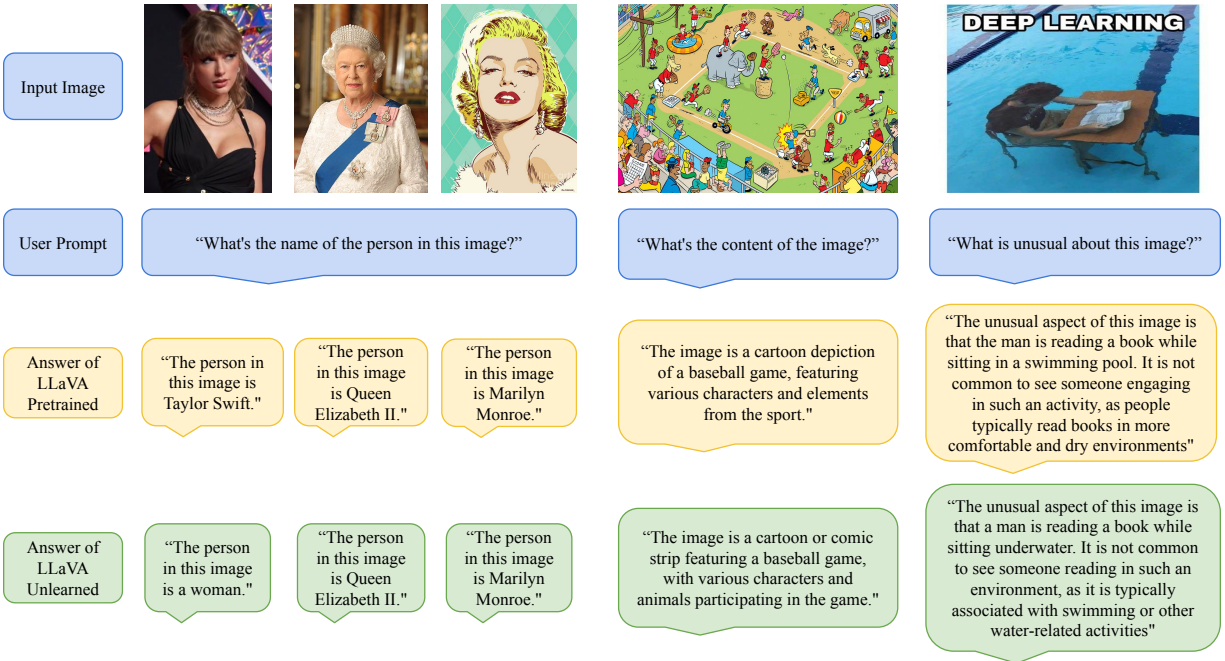


Figure 17: Qualitative evaluation on unlearning name "Taylor Swift" from LLaVA 1.5. While "Taylor Swift" is mapped to "woman" after the unlearning, the other female celebrity identification remain unaffected. Besides, model's robustness against style distribution shift is also preserved.

F Algorithm pseudo code

Algorithm 1 SLSGU: Single Layer Single Gradient Unlearning

Require:

- Forget set D_f and retain set D_r ;
- Original model F_θ with model weights θ ;
- The set of all layers in the model, as L ;
- Forget loss function $\mathcal{L}_{\text{forget}}$ and retain loss function $\mathcal{L}_{\text{retain}}$;
- Evaluation metrics forget accuracy FA and test accuracy TA.

Ensure: Unlearned model parameters θ_f

- 1: Calculate and store gradients $\nabla_\theta \mathcal{L}_{\text{forget}}(\theta, D_f), \nabla_\theta \mathcal{L}_{\text{retain}}(\theta, D_r)$ ▷ Single gradient calculation
 - 2: **for** each layer l in L **do**
 - 3: Importance(l) = $\|\nabla_{\theta_l} \mathcal{L}_{\text{forget}}(\theta, D_f)\|_2 / \|\theta_l\|_2$ ▷ Calculate layer importance
 - 4: Alignment(l) = $\cos(\nabla_{\theta_l} \mathcal{L}_{\text{forget}}(\theta, D_f), \nabla_{\theta_l} \mathcal{L}_{\text{retain}}(\theta, D_r))$ ▷ Calculate layer alignment
 - 5: **end for**
 - 6: $P = \mathbf{PO}(L, \text{Importance}, \text{Alignment})$ ▷ Pareto optimal algorithm 2
 - 7: $Q \leftarrow \emptyset$ ▷ Set of layers and their performances
 - 8: **for** each layer l in P **do**
 - 9: $\lambda_0 = \text{Importance}(l) / 10$ ▷ Initialize step size
 - 10: $(\lambda, \text{FA}, \text{TA}) = \mathbf{BS}(\lambda_0, l)$ ▷ Binary search algorithm 3
 - 11: $Q \leftarrow Q \cup \{(l, \lambda, \text{FA}, \text{TA})\}$
 - 12: **end for**
 - 13: $\text{FA}_{\min} = \min_{(l, \lambda, \text{FA}, \text{TA}) \in Q} \text{FA}$ ▷ Identify minimum FA
 - 14: $Q_{\min} = \{(l, \lambda, \text{FA}, \text{TA}) \in Q \mid \text{FA} = \text{FA}_{\min}\}$ ▷ Filter sets with minimum FA
 - 15: $(l^*, \lambda^*, \text{FA}^*, \text{TA}^*) = \arg \max_{(l, \lambda, \text{FA}, \text{TA}) \in Q_{\min}} (\text{TA})$ ▷ Select set with highest TA
 - 16: **return** $\theta_f = \theta - \lambda^* \nabla_{\theta_{l^*}} \mathcal{L}_{\text{forget}}(\theta, D_f)$
-

Algorithm 2 Pareto Optimal: $P = \mathbf{PO}(L, \text{Importance}, \text{Alignment})$

Require:The set of all layers in the model, as L ;

Layer importance and gradient alignment of all layers

Ensure: The set of Pareto optimal layers

```
1: Initialize  $P \leftarrow \emptyset$  ▷ Set of layers on the Pareto front is empty
2: for each layer  $l$  in  $L$  do
3:   ParetoDominant  $\leftarrow$  true
4:   for each layer  $l'$  in  $L \setminus l$  do
5:     if  $(\text{Importance}(l') > \text{Importance}(l) \text{ and } \text{Alignment}(l') < \text{Alignment}(l))$  then
6:       ParetoDominant  $\leftarrow$  false
7:       break
8:     end if
9:   end for
10:  if ParetoDominant then
11:     $P \leftarrow P \cup \{l\}$  ▷ Identified a Pareto optimal layer
12:  end if
13: end for
14: return  $P$  ▷ Return the set of Pareto optimal layers
```

Algorithm 3 Binary Search for Optimal Step Size: $(\lambda^*, \text{FA}^*, \text{TA}^*) = \text{BS}(\lambda_0, l)$

Require:

- Initial step size λ_0 ;
- Maximum number of steps K ;
- Model parameters θ ;
- Forget gradient of layer l : $G_l = \nabla_{\theta} \mathcal{L}_{\text{forget}}(\theta, D_{\text{f}})$

Ensure: Optimal λ^* , forget accuracy FA, test accuracy TA

```
1:  $\lambda_{\text{low}} \leftarrow 0$ 
2:  $\lambda_{\text{high}} \leftarrow \infty$ 
3:  $\lambda \leftarrow \lambda_0$ 
4:  $k \leftarrow 0$ 
5: Initialize  $P \leftarrow \emptyset$  ▷ Performance set
6: while  $k < K$  do
7:    $\text{FA}, \text{TA} = \text{eval}(\theta - \lambda G_l)$ 
8:    $P \leftarrow P \cup \{(\lambda, \text{FA}, \text{TA})\}$  ▷ Store results
9:   if  $\text{FA} > 0$  then
10:     $\lambda_{\text{low}} \leftarrow \lambda$  ▷ Should increase step size to unlearn
11:   else
12:     $\lambda_{\text{high}} \leftarrow \lambda$  ▷ Should reduce step size to avoid over-unlearning
13:   end if
14:   if  $\lambda_{\text{high}} == \infty$  then
15:     $\lambda \leftarrow 2\lambda$ 
16:   else
17:     $\lambda \leftarrow (\lambda_{\text{low}} + \lambda_{\text{high}})/2$ 
18:   end if
19:    $k \leftarrow k + 1$ 
20: end while
21:  $\text{FA}_{\text{min}} = \min_{(\lambda, \text{FA}, \text{TA}) \in P} \text{FA}$  ▷ Identify minimum FA
22:  $P_{\text{min}} = \{(\lambda, \text{FA}, \text{TA}) \in P \mid \text{FA} = \text{FA}_{\text{min}}\}$  ▷ Filter sets with minimum FA
23:  $(\lambda^*, \text{FA}^*, \text{TA}^*) = \arg \max_{(\lambda, \text{FA}, \text{TA}) \in P_{\text{min}}} (\text{TA})$  ▷ Select set with highest TA
24: return  $\lambda^*, \text{FA}^*, \text{TA}^*$  ▷ Select the set with lowest FA which has the highest TA
```
